DOI:10.12442/j.issn.1002-185X.20250367

Numerical simulations of dynamical relaxations in metallic glasses: a short review

Claudio Fusco

Univ. Lyon, INSA Lyon, CNRS, MATEIS, UMR5510, 69100 Villeurbanne, France

Abstract

Metallic glasses are a unique class of materials with exceptional mechanical properties, including high strength, excellent corrosion resistance, and significant elasticity. These materials display intriguing dynamical relaxation processes, which influence their mechanical and thermal properties. Understanding the dynamical relaxations in metallic glasses is crucial for optimizing their performance in various applications. Due to the limitations of experimental techniques to access processes at the atomic level, the detailed mechanisms responsible for the dynamical relaxations cannot be easily probed experimentally. Numerical simulations are good candidates to analyze in depth the elementary dynamical processes at the atomic scale and thus to capture the fundamental origin of dynamical relaxations. The development of computing power in the last decades has allowed researchers to reach an enormous advancement in the understanding of the physical mechanisms behind dynamical relaxations in metallic glasses.

This review provides a brief overview of the current state of research in numerical simulations of dynamical relaxations in metallic glasses, highlighting key methodologies, significant findings, ongoing challenges, and future directions. By synthesizing current research, this review emphasizes the importance of these simulations in improving the design and processing of metallic glasses for a wide range of applications, from structural materials to high-performance components.

I. INTRODUCTION

Metallic glasses (MGs) represent a fascinating class of materials with remarkable structural and mechanical properties due to the absence of long-range order, such as high toughness, exceptional mechanical strength, elastic deformation almost ten times larger than their crystalline counterparts and high corrosion resistance, making them a subject of study since the 90s [1–5]. For these reasons they are candidate materials in various areas, e.g. for micro-electromechanical systems [6], biomedical equipment applications [7], and as solar wind collectors [8] and spacecraft shielding [9], as well as for sport equipment. Due to their structural amorphousness MGs display a very complex dynamical and mechanical behavior, starting from the glass formation process up to their deformation mechanisms. The Achilles' heel of these materials is their low ductility at room temperature, which severely hinders their application as structural materials [10, 11]. Understanding and controling the brittle behavior and the lack of plasticity of MGs is one of the main challenges of the research on MGs [12]. Unlike crystalline solids, where plasticity can be described by the motion of dislocations, the elementary mechanisms of plasticity in MGs, and more generally in amorphous materials, are not completely established yet. One possible basic brick to understand the plasticity in glasses is the Shear Transformation (ST) or Shear Transformation Zone (STZ) concept [13], corresponding to

the region where irreversible atomic rearrangements take place, and possibly explaining the shear

banding phenomenon [14] leading to the catastrophic failure of glass materials. At the same time, plasticity in MGs is intrinsically linked to the disordered nature of glasses and to their relaxation behavior [15]. In fact, MGs are metastable, thermodynamically out-of-equilibrium structures, and their energy state is highly determined by the cooling history. Structural relaxation phenomena occur when the glass evolves from a high-energy to a lower-energy state [16]. A comprehensive understanding of these relaxation processes is essential for determining from a fundamental point of view the relationship between the glass dynamics and plasticity, and for improving the performance and reliability of MGs in practical applications.

So far, the mechanical properties and the dynamical relaxations of MGs have been studied by experimental techniques to a certain extent [3, 16–18]. However, experimental methods often face severe limitations for probing the atomistic mechanisms at the origin of plasticity and relaxation behavior, and to deeply understand phenomena such as shear banding, and the relationship between the local atomic structure and the observed mechanical behavior. In parallel, the computing power has enormously developed in the last decades, and consequently numerical simulations have emerged as a critical tool for investigating the properties of metallic glasses, providing insights into atomic-scale dynamics, mechanical response, and local structural features [19–21].

This review aims to summarize the current state of the art in numerical simulations of dynamical relaxations in metallic glasses, though in a non exhaustive manner, focusing on relevant methodologies, significant findings, challenges and future directions.

The paper is organized as follows. Sec. II provides some basic features and generalities of dynamical relaxations, emphasizing the unsolved issues and the limitations of experimental techniques to deeply investigate in detail the mechanisms at the origin of the different relaxation modes. Sec. III presents a very general overview of the main numerical methods used to study the dynamic processes and the structural heterogeneities in MGs, with a focus on the advantages and limitations of each technique. In Sec. IV, we summarize the key findings related to the dynamical relaxations, dynamical heterogeneities and viscoelastic behavior of MGs obtained by numerical simulations, highlighting their role to unravel the atomic-scale mechanisms governing the dynamical relaxations and to visualize the atomic dynamics, which are not accessible by experimental techniques. Sec. V is devoted to the conclusions and to the future perspectives opened by the use of numerical simulations to deeply investigate issues related to dynamical relaxations in MGs, paving the way for enhanced design in current applications.

II. GENERALITIES ON DYNAMICAL RELAXATIONS

MGs, as other amorphous materials, are characterized by a complex structural dynamics. Since MGs are metastable structures, their energetic state is determined by the thermo-mechanical history to which they are subjected. In particular, the cooling rate is an important parameter that influences the structure and energy level of a MG. When a MG is prepared in a high-energy state it can easily jump to a lower-energy state, and this phenomenon is called *relaxation*. Relaxation is a consequence of the disordered structure of a glass, lacking long-range atomic order. For example, in a crystal with dislocations or grain boundaries some weak relaxation modes can be observed. Since the atomic structure of the glass is highly disordered, we expect that its relaxation dynamics will be much more complex and intriguing than that of a crystalline system [22]. Moreover, the relaxation dynamics provides us with a direct link to the local atomic structure of the glass, thus studying the relaxation dynamics allows to probe the structural features of glasses. Relaxation is a consequence of the atomic dynamic behavior and can be activated by external stimuli such as applied stress or temperature change [17, 23], giving rise to mechanical or structural relaxation [17, 24, 25]. Relaxation can in principle also happen spontaneously, but this phenomenon called aging usually occurs on very long times scales of months or even years. MGs show complex relaxation dynamics, characterized by atomic processes responsible for different relaxation modes, and extending over a wide range of temperatures and frequencies [23, 25–27]. One of the main approaches to investigate the dynamical relaxations of MGs is to study their mechanical relaxation behavior, namely the response of the system to an external perturbation, such as an imposed deformation or an external stress [28, 29]. MGs represent a benchmark system in this respect, because they have more symmetric and less localized interactions with respect to other glasses, such as silica for instance, characterized by stronger localized bonding. In mechanical relaxation experiments the stress σ is monitored as a result of an imposed strain ϵ, and following the theory of viscoelasticity, the time or frequency dependence of the elastic modulus $M = \sigma/\epsilon$ can be obtained. In particular, in the time domain

$$M(t) = (\Delta\sigma\phi(t) + \sigma_r)/\epsilon, \tag{1}$$

where $\Delta\sigma$ represents the stress decay during relaxation, σ_r the remnant stress and $\phi(t)$ is the relaxation function. An example of mechanical relaxation technique is the Dynamical Mechanical Spectroscopy (DMS), which is an effective tool to probe the relaxation behavior due to its wide applicability and sensitivity to detect the atomic dynamics [24]. During a DMS test a sinusoidal

strain with amplitude ϵ_A and angular frequency ω of the form $\epsilon = \epsilon_A \sin(\omega t)$ is applied to the system and the resulting stress $\sigma = \sigma_A \sin(\omega t + \delta)$ is measured, where σ_A is the stress amplitude and δ is the phase shift. From these quantities the complex elastic modulus $M^*(\omega)$ can be obtained as

$$M^*(\omega) = (\sigma_A/\epsilon_A)(\cos\delta + i\sin\delta) = M'(\omega) + iM''(\omega) \quad (2)$$

where $M'(\omega)$ and $M''(\omega)$ are called *dynamic moduli* and represent the storage and loss modulus respectively. The storage modulus is related to the energy that is stored and released in one loading cycle and is of purely elastic origin, while the loss modulus is proportional to the energy dissipated in one cycle due to viscosity or phase transitions. Thus, DMS can completely characterize the viscoelastic behavior of the material. The dynamic moduli are often combined in one single variable called internal friction or loss factor:

$$\tan\delta = M''/M' \quad (3)$$

In Fast Scanning Calorimetry experiments the dynamical moduli are studied as a function of temperature variation in order to identify the characteristic temperatures where relaxations occur (thermally activated relaxations). The relaxation modes that are usually observed in MGs are the α, or main relaxation, and the β, or secondary relaxation. These two processes are associated to different kinds of atomic rearrangements leading to different dynamical relaxations. The α relaxation is a large-scale structural rearrangement, which usually exists in supercooled liquids, above T_g, and becomes frozen below T_g. When the supercooled liquid is cooled approaching T_g the dynamics becomes very sluggish and the α relaxation time τ_α can increase by many orders of magnitude when the temperature just decreases by few degrees near T_g from above. In fact, the relaxation function $\phi(t)$ for a supercooled liquid near T_g does not follow an exponential decay as in a classical liquid, but a stretched exponential behavior $\phi(t) \sim \exp[(-t/\tau_\alpha)^\beta]$, where β is the stretching exponent smaller than 1 for most glass-formers, indicating the dynamics is slower than that of a liquid [30]. Interestingly, $\tau_\alpha(T)$ follows a VFT law for an equilibrium supercooled liquid near T_g, and is described by an Arrhenius behavior in the glassy region far below T_g, where the glass is out of equilibrium [28, 31]. When the glass is cooled below T_g another dynamical relaxation mode, called β relaxation, starts to appear, becoming dominant when temperature is further decreased. Unlike the α relaxation, the β relaxation is associated to local structural rearrangements and does not strongly depend on temperature. The features of dynamical relaxations can be represented by two distinct peaks in the DMS spectra as a function of temperature, as it can be seen for example

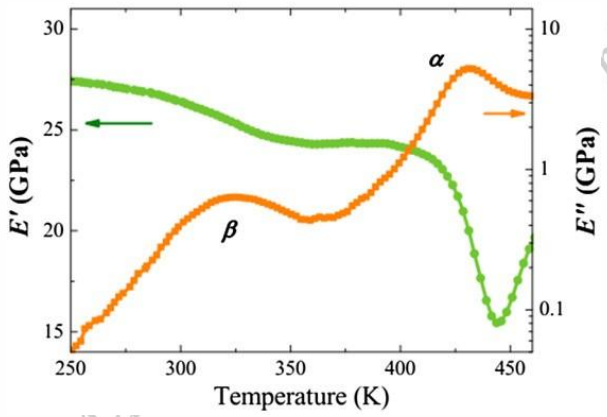

FIG. 1. Temperature-dependence of storage and loss moduli for $La_{68.5}Ni_{16}Al_{14}Co_{1.5}$ MG. The α and β relaxation peaks are clearly visible. Reprinted with permission from Ref. [25], copyright (2014).

in Fig. 1 where the α peak is located at a high temperature, close to T_g, while the β peak occurs at lower temperatures, usually of the order of $0.7 - 0.9T_g$ for most MGs. The α relaxation peak occurs over a wide range of frequencies, depending on the temperature of the sample, typically from 10^{-3} to 10^{2} Hz. As shown in Fig. 2, the α peak shifts to higher temperatures when the frequency increases, and the frequency scales with the exponential of the inverse of the temperature of the α peak. It is worth noticing that while the main α relaxation peak is observed in all MGs, the β relaxation does not occur in the same way in all MGs: sometimes the β peak is not observed, or alternatively only an excess wing can be seen in the DMS spectra, and sometimes it is hardly visible. The conditions by which the β relaxation manifests itself in MGs is one of the main puzzles related to the physics of MGs and has been the subject of different works [24, 25, 32–35].

Compared to the α relaxation, β relaxation demonstrates low amplitude but a more comprehensive temperature range which indicates its wide distribution of relaxation times. Different studies suggest that these two relaxation modes are not completely independent and that for example β relaxation acts as a precursor of α relaxation in some situations [16, 36–39]. In fact, when temperature increases close to T_g, the β relaxation wing gradually merges into the α relaxation peak. manifesting the connection between the two types of dynamic behaviors. In the perspective of the potential energy landscape, the β relaxation corresponds to small scale hopping events between neighboring energy minima, while the α relaxation is associated to configurational transitions from one megabasin to another [24, 40], as illustrated in Fig. 3. Unlike the large-scale collective rearrangements occurring during the α relaxation, the β relaxation is associated with local structural atomic motion, as depicted in Fig. 4(b)-(c). The mystery of β relaxation has not been totally

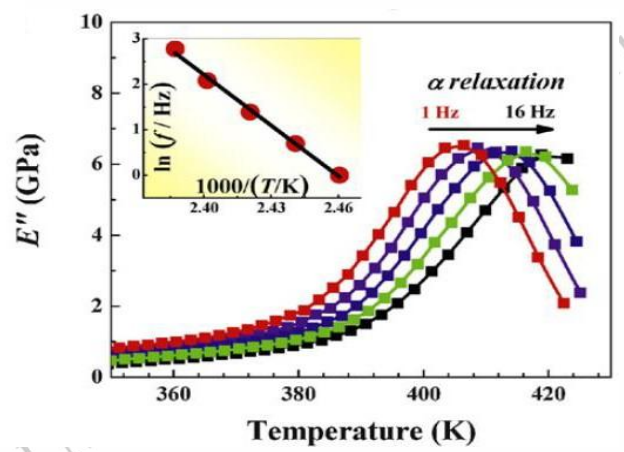

FIG. 2. Temperature dependence of the loss modulus for $Ce_{0.2}La_{0.8}Al_{10}Cu_{20}Co_2$ MG showing the α relaxation peak for different frequencies. The inset is a plot of the frequency vs. the α peak temperature with an Arrhenius fit. Reprinted with permission from Ref. [24], copyright (2013).

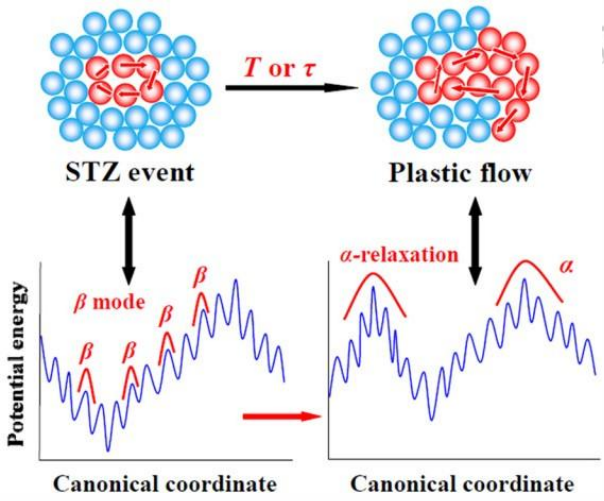

FIG. 3. Schematic representation of the β and α relaxations in the potential energy landscape. Reprinted with permission from Ref. [41], copyright (2015).

unveiled, although recent studies have identified its basic mechanism and its correlation with the α relaxation [22]. It has been shown that β relaxation has a close correlation with other dynamic processes in MGs and that can be of primary importance to understand the structural and mechanical characteristics of MGs [12, 32, 33, 43, 44]. The relaxation process and characteristics are highly affected by the structural nature of the glass materials and in particular by the chemical composition, as first pointed out by Wang for La-based MGs [45]. Yu et al. [46] proposed that β relaxation is associated with regions where all the atomic pairs have large similar negative values

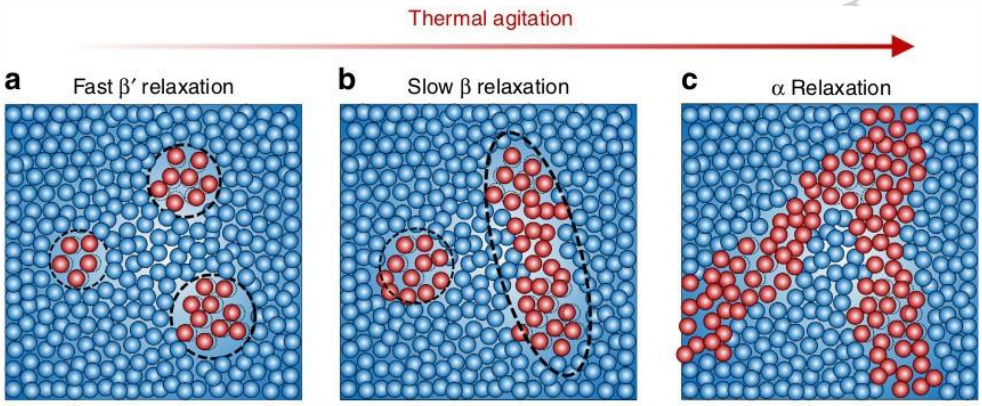

FIG. 4. Pictorial atomic mechanisms associated to the different relaxation modes: (a) the fast β' relaxation is due to local non-affine atomic displacements; (b) the slow β relaxation is associated to local structural rearrangements; (c) the α relaxation is characterized by the percolation of local relaxations spanning the entire system. Reprinted with permission from Ref. [42], copyright (2015).

of mixing enthalpy. Additionally, the effect of atomic pairs on the relaxation behavior is not only determined by their atomic properties, but also depends on their specific chemical environments and interactions with other atoms [24, 46]. Furthermore, Huang et al. remarked that a more pronounced β relaxation peak occurs when the boson peak, e.g. the excess of vibrational density of states, is stronger [47]. The cooling process of the glass material, as well as the aging history, also plays an essential role in the relaxation dynamics. For example, slow quenching can make the glass more stable than the fast quenched system hence reducing the intensity of β relaxation in MGs, even if it can never totally suppress the relaxation [24, 48]. Works by Yu et al. [24] and Rodney and Schuh [49] showed that the activation energy of the β relaxation is equivalent to the energy barrier of a Shear Transformation Zone (STZ), i.e. an elementary plastic rearrangement, indicating a close correlation between this relaxation mode and plasticity, or inhomogeneous local atomic motion, in MGs. Thus, to a certain extent, the deformation mechanisms of MGs can be altered by controlling the β relaxation. The modulation of the β relaxation can tailor the structural inhomogeneities of the MGs and tune the macroscopic flow, eventually enhancing ductility [17]. Generally, the β relaxation can be modulated by designing optimal compositions of MGs, by changing the cooling rate and by applying a non-affine strain to the system [33, 50–52]. For instance, in the La-based MG with a proper addition of Ni and Al a strong β relaxation peak is observed compared to a traditional Cu-based MG, as shown in Fig. 5. As it can be seen in the mechanical stress-strain curves in Fig. 6, the La-based glass has a better tensile plasticity, while the behavior of the Cu-based MG is more brittle.

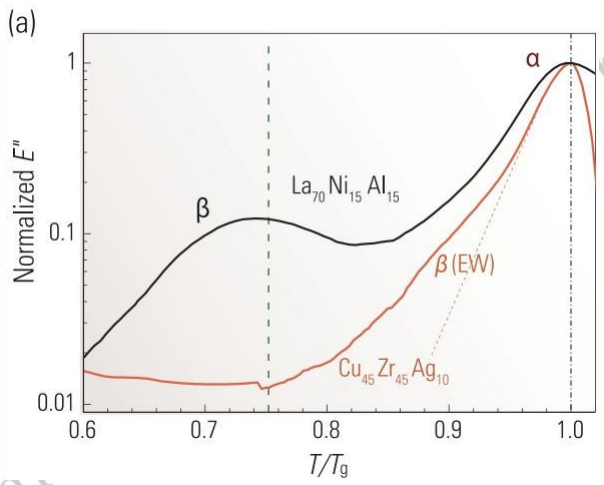

FIG. 5. Temperature dependence of loss modulus for two different MGs. In the La-based MG the β relaxation is much more pronounced than in the Cu-based MG. Reprinted with permission from Ref. [53], copyright (2014).

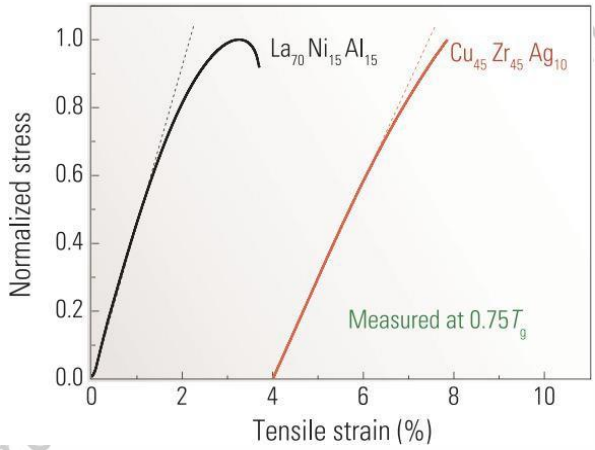

FIG. 6. Stress-strain curve for two different MGs. While the La-based MG overcomes the yield stress, the behavior of the Cu-based is more brittle. Reprinted with permission from Ref. [53], copyright (2014).

Beyond the significant primary α of secondary β relaxations, a third relaxation mode, called fast β relaxation, or β' or γ relaxation was observed very recently [42, 54–57]. This process occurs at very low temperatures, in the range of 0.2-0.3 T_g and it can be seen as an extra small peak in the DMS spectra, as for example in Fig. 7, with a lower activation energy than that for the slow β relaxation. It is generally believed that it is associated to a non-affine atomic rearrangement arising from atomic-level thermal stress generated during cooling [57], as pictorially illustrated in Fig. 4(a). However, the underlying physical mechanisms of this process remain unclear and further analysis has to be done in order to have a deeper understanding of this relaxation mode.

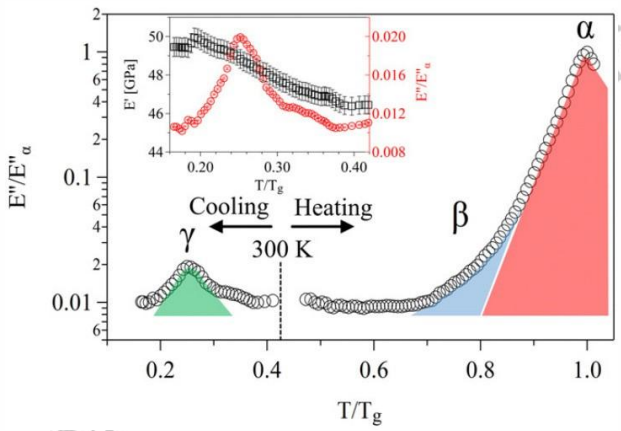

FIG. 7. Temperature dependence of normalized loss modulus for $Zr_{58.5}Cu_{15.6}Ni_{12.8}Al_{10.3}Nb_{2.8}$ where three different relaxation modes can be observed. The inset shows a zoom of the storage and loss moduli in the temperature region of the γ relaxation mode. Reprinted with permission from Ref. [57], copyright (2017).

III. NUMERICAL SIMULATION METHODS

Different simulation techniques are used to study materials' properties, depending on the relevant time and length scales on which the phenomena of interest are probed. In this section we introduce two basic simulation methods used to investigate the structure and the dynamical relaxations, as well as the mechanical behavior of MGs, namely Molecular Dynamics (MD) and Monte Carlo (MC).

A. Molecular Dynamics simulations

MD is a widespread technique to study the mechanical behavior of MGs and glasses in general since it can shed light on the atomic structure and on the atomistic processes responsible for the mechanical behavior of MGs, which cannot be entirely probed by experimental techniques [19].

1. General principles

MD is a computational method that can simulate the time-dependent behavior of particles and generate atomic positions and velocities by numerically solving the Newton's equations with given initial conditions [58, 59]. In this sense, MD is a deterministic technique and the dynamic process has a time-reversal symmetry [60]. In order to integrate the equations of motions an interaction potential between the particles has to be specified in order to obtain the interatomic forces used in the Newton's equations. The choice of a proper interatomic potential that can reliably describe the

structure and the physical properties of the system is one of the main challenges of MD simulations, as explained in more detail in Sec. III A 2. In general, the accuracy of MD simulations depends on the initial configuration, on the value of the integration timestep (usually of the order of 1 fs) and on the interatomic potential energy.

Since MD simulations focus on microscopic quantities (positions and velocities of particles), it is useful to define a Gibbs ensemble in order to predict the macroscopic properties of a large system based on the average of a large number of possible microstates. Depending on the experimental conditions of interest, a relevant ensemble should be defined. For example, an isolated system corresponds to the microcanonical ensemble (NVE). However, an isolated system does not always mimic practical experimental conditions: in experiments the system is either in contact with a heat bath or has an imposed pressure or both. Thus, a closed isothermal system correponds to the canonical ensemble (NVT) or to the isothermal-isobaric ensemble (NPT) [61]. Typically used thermostats and barostats in MD are those of Nosé-Hoover, consisting in adjusting the atomic velocities to reach a target temperature for the thermostat [62], and to adjust the system volume to reach a target constant pressure for the barostat [58].

2. *Interatomic potentials*

One of the indispensable parts of classical MD simulations is the potential energy describing the interaction between particles in the system [63]. While in *ab-initio* MD simulations the interatomic interactions are based on first-principle calculations, classical MD simulations rely on empirical interatomic potentials describing the interactions between the atoms. Many studies of metallic glasses have used simple pair potentials such as the Lennard-Jones potential [64–66]. In spite of their simplicity, the simulations based on these potentials can provide significant insight on some physical properties of the glass transition and on the relaxation behavior [67]. However, pair potentials have intrinsic limitations when applied to metallic systems. For example, systems described with pair potentials always satisfy the Cauchy relation $C_{12} = C_{44}$ between elastic constants, whereas metallic systems typically strongly disobey the Cauchy relation [68]. In addition, pair potentials cannot describe the volume dependency of potential energy, which is known to be important in metallic systems [69]. Thus, it is essential to include many-body interactions to study the relaxation behavior of metals and metal alloys in a more realistic way. A commonly used interatomic potential for MGs is the Embedded Atom Method (EAM) potential [70]. In this model the total energy U_i of atom i

is given by

$$U_i = F_\alpha \left(\sum_{j \neq i} \rho_\beta (r_{ij}) \right) + \frac{1}{2} \sum_{j \neq i} \Phi_{\alpha\beta}(r_{ij}) \quad (4)$$

where α and β are the atom types, F is the embedding function, i.e. the energy to place atom i of type α in the electronic cloud of the other atoms described by the electronic density ρ, and Φ is a pair-wise potential function. Usually the sum in the Eq. (4) is performed on all atoms located within a cutoff radius r_c, assuming a zero energy when the distance between two atoms exceeds r_c. The parameters F, ρ and Φ are optimized for a given material in order to match with experimentally measurable properties, such as density, lattice parameters, elastic constants, cohesive energy, melting point, bulk modulus etc., or in some cases with properties that can be obtained by ab-initio MD simulations. A widely used parametrization of the EAM is given by the Mendelev potential [71], which is employed for instance for the CuZr binary alloy, a prototypical material model studied by MD simulations for its simplicity. Another type of multi-body potential is represented by the Sutton-Chen (SC) potential, which is a long-range Finnis-Sinclair potential with a simple power law form:

$$U_i = \frac{1}{2} \sum_{j \neq i} \epsilon_{ij} V(r_{ij}) - c_i \epsilon_{ii} \rho_i^{1/2} \quad (5)$$

where $V(r_{ij}) = (\alpha_{ij}/r_{ij})^n$ is a repulsive pair potential between atoms i and j due to Pauli's repulsion between electronic clouds, $\rho_i = \sum_{j \neq i} (\alpha_{ij}/r_{ij})^m$ is a local energy density of atom i, ϵ sets the overall energy scale, c_i is a dimensionless parameter and α is a typical length parameter. As for the EAM potential, the parameters of the SC potential can be optimized to reproduce experimental properties [72] or can be obtained by fitting the results of first-principle ab-initio calculations. For example, Landa et al. proposed a parametrization of the empirical many-body SC potential for Pb-Bi and Pb-Ni systems using both experimental data and physical quantities derived by ab-initio calculations [73], and Faruq et al. used first-principle calculations to fit the SC potentials for the Pd-Si system [74] . Finally, the Second-Moment Approximation of the Tight-Binding scheme (TB-SMA) is an empirical interatomic potential vastly employed in the literature for metallic systems, especially for transition-metal alloys. In this model, the potential energy of atom i, U_i is written as the sum of a repulsive term, $U_{i,R}$ and an attractive term $U_{i,B}$:

$$U_i = U_{i,R} + U_{i,B} \quad (6)$$

where

$$U_{i,R} = \sum_j A_{\alpha\beta} \exp\left[-p_{\alpha\beta} \left(\frac{r_{ij}}{r_0^{\alpha\beta}} - 1 \right) \right] \quad (7)$$

and

$$U_{i,B} = \sum_{j} \xi_{\alpha\beta}^{2} \exp\left(-2q_{\alpha\beta}\left(\frac{r_{ij}}{r_{0}^{\alpha\beta}} - 1\right)\right)^{1/2} \quad (8)$$

α and β are atom types, $r_0^{\alpha\beta}$ is the first-neighbor distance, $\xi_{\alpha\beta}$ is an effective hopping integral, $A_{\alpha\beta}$ is a constant depending on the experimental values and $p_{\alpha\beta}$ is related to the compressibility of the bulk material. TB-SMA potential has been used to simulate the glass-forming ability of binary Ti-Co alloys [75], the dynamic properties of PdAuPt ternary nanoparticles [76], the mechanical properties of CuZrTi MGs [77], and the structure and glass-forming ability of CuZrCo MGs [78]. The parameters of the TB-SMA potential for these systems were optimized and adjusted by Cleri and Rosato to reproduce cohesive energy, density and elastic constants of the real systems [79].

We further notice that while the number of parameters in the empirical potentials used to describe binary alloys are rather limited, as soon as the number of elements starts to increase the description of the interatomic interactions between different pairs of elements become increasingly complex since the number of parameters that have to be optimized scales with the square of the number of elements [80]. Moreover, a given parametrization of an interatomic potential is often developed for a certain range of temperatures and pressures and for a given glass composition, so that the transferibility to other experimental conditions is not always guaranteed [81].

3. *Molecular Dynamics for DMS*

In order to perform MD simulations of DMS to study dynamical relaxation in metallic glasses, first a metallic glass structure has to be created. One of the most common methods to prepare a glass by MD is the melt-quenching process that reproduces in a computer experiment the real experimental process of glass preparation [82], schematically illustrated in Fig. 8. Once the interatomic potential and the simulation box dimensions have been chosen, usually imposing periodic boundary conditions (PBC) to simulate a bulk sample, the first step is to prepare an initial configuration, for example a crystalline structure if the crystal with the same composition as that of the glass exists, or alternatively a random distribution of atoms [61]. The number of atoms and the box dimensions are sually chosen to match the experimental density of the glass. Then, the initial configuration is heated up to high temperature T_{high} (higher than the melting point) in order to completely melt it. At this point, the system is stabilized for a certain annealing time in order to equilibrate the liquid sample. After this equilibration time, the sample is cooled down with a constant cooling rate up to a low temperature T_{low}. The cooling process can be performed in the NVT or in the NPT ensemble,

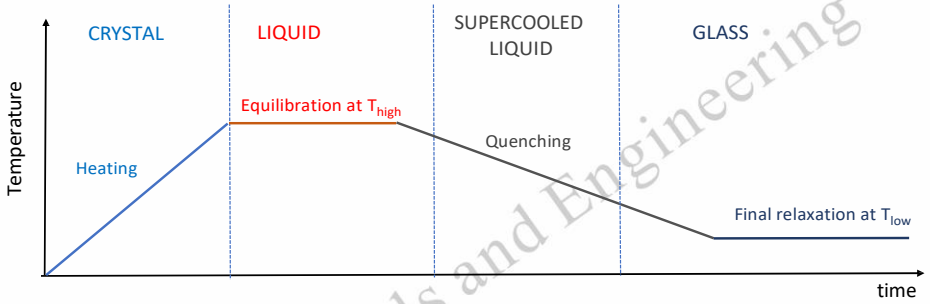

FIG. 8. Scheme of a melt-quenching simulation. The initial configuration is heated up to high temperature, equilibrated at this temperature, then cooled down at low temperature and relaxed at this temperature.

the latter being closer to the experimental procedure of glass preparation. Typical values of cooling rates used in MD simulations are between 10^{8} and 10^{14} K/s, much larger than the experimental cooling rates. The system is then relaxed at the temperature T_{low} for a certain time (usually few ns are enough) in order to create a stable glass structure. It is possible to estimate the glass transition temperature T_g by plotting the evolution of the internal energy, or the enthalpy, or the volume of the simulation box as a function of temperature during the cooling process, and identifying the point where the slope of the curve drastically changes. If the potential energy is monitored as a function of time a plateau reached during the relaxation signals that the glass structure is well stabilized. Furthermore, some structural analysis, including coordination number, pair distribution function or structure factor, can be useful to asses the amorphous character of the glass [58, 83]. In order to achieve a statistically well relaxed glass structure, sometimes it is useful to perform the melt-quenching procedure several times, and average the results obtained by different simulations. In order to simulate DMS by MD at different temperatures the glass is first heated at the target temperature and then isothermally equilibrated at this temperature and with zero pressure for few nanoseconds [25, 84, 85]. Then, an oscillatory strain of the form $\epsilon_{xx} = \epsilon_A \sin(\omega t)$, where $\omega = 2\pi/T_\omega$ (T_ω being the period of the applied strain) is applied for instance in the x direction. The amplitude ϵ_A has to be small enough to ensure that the glass remains in the elastic regime, but not too small to prevent a too low signal-to-noise ratio. Typically, $\epsilon_A \sim 1\%$ is an optimal value. Different loading conditions can be applied, for example constant-volume, uniaxial, longitudinal or isostatic deformation [86]. The resulting stress σ_{xx} in the x direction is monitored and fitted by a sinusoidal function, $\sigma_{xx} = \sigma_0 + \sigma_A \sin(\omega t + \delta)$, where σ_0 is a small offset used to increase the numerical accuracy of the fit. The dynamic moduli and the loss factor are then obtained by Eqs. (2) and (3). Several cycles are often performed to obtain a more accurate estimation of the dynamic moduli. Fig. 9 shows an example of a DMS cycle where a sinusoidal strain is applied under constant-volume conditions and

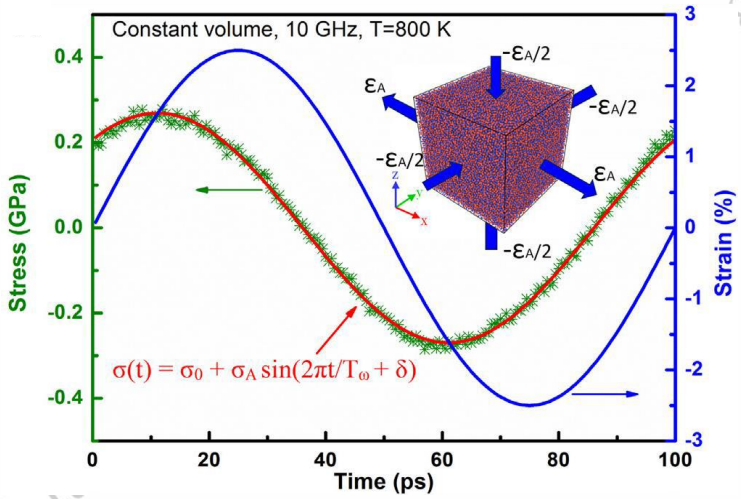

FIG. 9. Applied sinusoidal strain with amplitude of 2.5% and frequency 10 GHz, and resulting measured stress for a constant volume deformation implemented by MD simulations of DMS at 800 K for $Cu_{64}Zr_{36}$. The inset shows an atomic configuration with a scheme of the loading condition. Reprinted with permission from Ref. [86], copyright (2020).

the stress is fitted by a sinusoidal function. The stress curve contains a certain level of noise that can be reduced by either increasing the number of cycles or increasing the amplitude ϵ_A, provided that the deformation remains in the elastic regime. Notice that the typical values of the frequencies accessible to MD simulations range from 1 GHz to 100 GHz, several orders of magnitudes higher than the experimental frequencies that usually do not exceed few kHz.

4. *Strengths and limitations*

MD is a useful technique to study complex systems such as MGs since it can provide atomic-level insights on phenomena occurring at the molecular scale, allowing to rationalize the atomistic mechanisms at the origin of various physical processes. For example, MD studies on the glass-forming ability have identified the role of atomic size effects [87] and the correlation between atomic structure and transport properties [88]. It has also been possible to shed light on the deformation mechanisms of MGs unravelling some features of the STZs nucleation and shear band formation [89, 90]. Concerning dynamical relaxations, the role of Short-Range Order (SRO), namely the distribution of icosahedra clusters, on the α relaxation behavior was pointed out by MD simulations [91]. The atomistic mechanisms responsible for the β relaxations have also been identified by several works by Yu et al. as string-like motion [24, 25, 34, 35]. Recent studies by MD simulations have allowed

to trace the origin of dissipation in MGs and to connect the atomic mobility to the local microstructure [86]. More details about specific achievements in the understanding of dynamical relaxations in MGs by MD simulations will be presented in Sec. IV.

In spite of the possibilities offered by MD to describe phenomena at the atomic scale, many limitations have still to be overcome. The first limitation concerns the timescales accessible to MD simulations. In fact, the simulation's time duration depends on the integration timestep, which should be small enough to avoid discretization errors in the integration of the atomic equations of motion, and the sum of the timesteps must be large enough to capture the effect being modeled in a reasonable time. A typical value of the timestep is of the order of 1 fs. Therefore, the timescale of MD simulations is often limited to the picoseconds to few hundreds of microseconds range. For example, as already mentioned in Sec. III A 3, the cooling rates used in MD simulations are much higher than the experimental ones, thus creating a systematic difference between experimental and simulated glasses [92], and often resulting in not well-relaxed glass structures. Moreover, when simulating deformation, extremely high strain rates, usually higher than $10^7\ s^{-1}$ are applied to the system, and in cyclic deformation, like those used to simulate DMS, the frequency of the the applied cycle is also very high compared to experimental values, as already pointed out in Sec. III A 3, often resulting in high yield stress compared to those found in experiments.

In order to overcome the timescale limitations of standard MD, some approaches coupling MD to other sampling methods have been proposed. The so-called metadynamics is one of these methods allowing to enhance sampling of rare events and explore free energy landscapes of a system, particularly useful for systems with barriers that are difficult to cross within standard MD timescales [93]. This method is very practical because it allows to reduce the dimensionality of a large systems with $3N$ degrees of freedom, N being the number of particles in the system, to one or two degrees of freedom, called collective variables (CVs), which describe the system's essential dynamics, for example the distance between atoms or molecular groups, bond angles, or the principal components of atomic positions. However, a proper choice of appropriate CVs is critical, since poor CVs choices can limit exploration or bias the results. Furthermore, a time-dependent bias potential is added to encourage the system to explore configurations that are rarely visited under standard MD. The bias "fills in" free energy minima as the simulation progresses, allowing the system to escape these traps. After sufficient sampling, the accumulated bias potential approximates the free energy landscape. The analysis of this landscape allows to identify the stable states, to compute the energy barriers and to study the sequence of explored configurations in order to understand reaction pathways, transitions, and mechanisms. Different variants of metadynamics have been proposed, such as well-tempered

metadynamics [94], parallel bias metadynamics [95] and bias-exchange metadynamics [96].

Another limitation of MD simulations concerns the accessible length scale. Due the high computational cost, MD simulations are limited to small systems, with linear dimensions up to few tens to nanometers. With the dramatic development of computer power, the sample size can nowadays reach millions of atoms. Although PBC are used to simulate bulk systems, the limited size of simulated glasses can affect the accuracy of the simulations [80], for instance leading to poor statistical sampling [97] and to large fluctuations in the thermodynamic properties for too small systems [98].

B. Monte Carlo techniques

MD is the most common simulation method to probe the dynamics at the atomic scale and thus to study dynamical relaxations in glasses. However, due to the timescale limitations of this technique explained in Sec. III A 4, other accelerated simulation methods have been proposed in order to fully explore the potential energy landscape and to overcome the potential energy barriers in an accessible timespan in order to find the potential energy minimum [99]. One of the simplest and most used techniques of this kind is the energy-based MC.

1. General principles

The MC method consists in randomly chosing an atom in a simulation box containing N atoms and try to move it randomly in the box within a certain maximum fixed distance in all directions. This move is accepted or not following a given acceptance rule [58, 100]. One of the most used acceptance rules is the Metropolis algorithm, which is based on an energy criterion. If the energy of the system in the present configuration is E and the energy of the system after attempting a random move of an atom is E', the move is accepted with the following probability [58]:

$$P = \begin{cases} 1 & \text{if } E' \leq E \\ \exp[-(E' - E)/k_B T] & \text{if } E' > E \end{cases} \quad (9)$$

In practice, if the energy of the system after the move decreases the move is always accepted, otherwise a random number ξ is generated uniformly between 0 and 1 and it is compared to $\exp[-(E' - E)/k_B T]$: if $\xi < \exp[-(E' - E)/k_B T]$ the move is accepted. Usually, one MC timestep corresponds to N attempted moves. The maximum allowed displacement of an atom during a move is an important parameter that has to be carefully chosen: it has to be neither to small to avoid the acceptance of a large number of moves and thus a little exploration of the phase space, neither

too large since most of the moves will be rejected. In practice, this parameter is adjusted during the simulation to yield an acceptance ratio of approximately one half of the moves [58].

The MC method allows to accelerate the exploration of the phase space and of the potential energy landscape with respect to MD, thus allowing to obtain better relaxed glasses [101, 102]. Different variants of the MC method have been proposed to enhance the performances of this technique. Some examples are illustrated in the next subsection.

2. Reverse Monte Carlo and Swap Monte Carlo

Refinements and variations of the MC technique have been suggested to improve the agreement with the experimental glass structure and to speed up the convergence to a minimum energy state. Concerning the first point, Reverse Monte Carlo (RMC) method was introduced two decades ago [103] in order to overcome the drawbacks of simple MC simulations often generating *in silico* structures not matching the experimental ones. In fact, the basic principle of RMC is the same as that of MC with the extra feature that the resulting glass structure has to satisfy some constraints imposed by experiments [104], eventually yielding more realistic structures. Specifically, a cost function is defined as related to the difference between the simulation results and the experimental reference, for instance for the pair distribution function that yields a global characterization of the atomic structure of the system [105]. The objective of RMC is to minimize this cost function by using a Metropolis-like algorithm [106] and therefore to provide atomistic structures in very good agreement with experimental data. As such, RMC can be used to construct atomic structural models of MGs [107, 108] and can offer a practical tool to model glass structures and dynamical relaxations when reliable experimental data are available [109].

Regarding the second point, i.e. a faster convergence to a minimum state in the potential energy landscape, we mention the Swap Monte Carlo (SMC) algorithm, which provides an efficient way to produce equilibrium configurations of a supercooled liquid [20, 101, 110] with effective equilibration times much lower than the experimental structural relaxation time. Besides attempting to displace particles, as in the standard MC, in SMC an extra move can be applied, consisting in exchanging the diameters of two randomly chosen particules, or equivalently their positions, with an acceptance rule based on the Metropolis criterion. It can be shown that this method respects the detailed balance principle and can therefore yield a final equilibrium state [111]. The frequency of the swap moves and the range of particle diameters for which the swap can be attempted can be tuned to optimize the efficiency of the SMC method. The SMC was first introduced to study hard-sphere

systems [112] and was then extended to investigate the glass transition of a binary mixture of soft spheres [113]. More recently, Ninarello et al. used SMC simulations to analyze the role of different features, like size polydispersity, particle softness, nonadditivity of interactions, for both discrete and continuous mixtures [110]. They found a gain up to 10 orders of magnitude in the equilibration time with respect to the standard MC method, even close and below T_g, thus allowing to measure physical properties over a wide range of temperatures under experimental conditions.

The swap Monte Carlo algorithm can be also implemented within a MD framework, replacing the swap moves by an exchange between the system and a reservoir of particles [101, 114–116].

3. Strengths and limitations

MC-based simulations are an interesting alternative to MD simulations to overcome the limitations of the melt-quenching procedure in order to generate glass structures that do not depend on the choice of the cooling rate. However, these simulations are not necessarily physically based and they cannot capture the spontaneous evolution of the system towards lower-energy states, thus generating structures probably very far from those of real experimental glasses [117]. While RMC simulations can provide a means to obtain glass structures matching experimental available data, their limitation is due to their inability to provide a physical insight in the dynamics of the atoms in a glass, as compared to MD simulations [118, 119]. Moreover, the method of RMC simulations to minimize the cost function is intrinsically ill-defined, since a given indicator, for example the pair distribution function, which is a one-dimensional signature, can be associated with several different three-dimensional structures [118]. Overall, SMC simulations on the contrary do not rely on the minimization of a cost function to match the obtained structures with experimental data, and can produce *in silico* glasses with an efficient sampling of the phase space especially for polydisperse systems. In systems with identical or nearly identical particles, however, swapping may not lead to significant configurational changes. This limits the utility of the method because the swaps do not meaningfully enhance exploration of the phase space [20]. Moreover, systems with strong structural constraints, such as ordered crystals or networks, may not benefit from swapping because proposed swaps often lead to energetically unfavorable configurations that are likely to be rejected [110]. At very low temperatures, swap moves are often rejected because they tend to increase energy significantly. This makes Swap Monte Carlo less effective for studying systems near their ground state or in highly ordered regimes. Careful consideration of system properties and combining swap moves with complementary techniques can help mitigate these limitations.

In conclusion, MD and MC represent two different and complementary techniques both very useful to understand different aspects of the relaxation dynamics in metallic glasses, and more generally in amorphous glassy materials. However, MD has been largely predominant in several works to investigate dynamical relaxations. In fact, since the relaxation is essentially a kinetic, non-equilibrium phenomenon, MD simulations are more suitable to study the non-equilibrium dynamics of amorphous solids with respect to MC simulations that were originally developed to investigate the equilibrium properties by performing configurational averages of thermodynamic quantities, or to study the static structure of liquids for instance. However, in the last two decades, MC simulations were increasingly used also beyond the structure and the thermodynamics, with the development of more sophisticated approaches based on local moves and algorithms going beyond the Metropolis acceptance rule, and allowing to more efficiently and rapidly sample the phase space when approaching the glass transition temperature [120]. Local MC can thus be considered as an efficient alternative to MD to sample not only static but also dynamic properties of supercooled liquids [20], allowing to reach much longer times and to study the long-time dynamics otherwise inaccessible by simple MD simulations. However, the drawback of MC approaches is that they often produce unphysical trajectories in the phase space in order to achieve a faster sampling. That is the reason why MC is used to produce well-equilibrated initial configurations of supercooled liquids which serve as input to MD simulations to further study dynamic relaxations at lower temperature. Moreover, the use of MD simulations can also provide a closer physical understanding of the atomic-scale features and mechanisms at the base of the different relaxation modes and to mimic the experimental DMS technique to investigate the viscoelastic properties of metallic glasses, which would be less straightforward by employing MC techniques.

IV. KEY FINDINGS ON DYNAMICAL RELAXATIONS BY NUMERICAL SIMULATIONS

In this section, we review, though in a non-exhaustive manner, some of the main contributions of numerical simulations studies to the physical understanding of dynamical relaxation in MGs.

1. Primary relaxation

The slowing down of the dynamics when cooling down a liquid near the glass transition temperature is one of the main features of the α relaxation process that calls for an atomistic understanding, which has therefore been the subject of several numerical studies focussing on the atomic-scale dynamics of a supercooled liquid near T_g. The relaxation dynamics can be characterized by the relaxation function $\phi(t)$ defined in Eq. (1). Usually, in computational studies, the relaxation function is assimilated to the self-part of the intermediate scattering function (SISF) $F_s(q, t)$, which characterizes the single-particle dynamics of a system of N particles [110]:

$$F_s(q,t) = \left\langle \frac{1}{N} \sum_j \exp(i\mathbf{q}\cdot[\mathbf{r}_j(t) - \mathbf{r}_j(0)]) \right\rangle \tag{10}$$

where $\mathbf{q}$ is the wave vector, usually corresponding to the first peak of the static structure factor, and $\langle\cdots\rangle$ denotes an ensemble average. It is known that for liquids the relaxation occurs in an exponential fashion, i.e. $\phi(t) \sim \exp(-t/\tau)$, while for supercooled liquids a stretched exponential behavior, given by the Kohlrausch-Williams-Watts (KWW) equation, i.e. $\phi(t) \sim \exp(-t/\tau)^\beta$, where β is the stretching exponent, is usually found [121]. The exponent $\beta < 1$ for most glass-forming liquids, signaling a stretch relaxation due to a more sluggish dynamics [23]. So far, the origin of the stretching behavior is not clearly established, and it is believed that it is either a consequence of the dynamical heterogeneity in different regions of spaces or a result of local relaxation [122, 123]. In a recent study, Shang et al. investigated this debated issue by MD simulations of a binary Lennard-Jones mixture subjected to a sinusoidal strain mimicking a DMS experiment [124]. They defined local elastic moduli by letting only a region of the sample of given size relax in isothermal conditions and measuring the local stress in this region. They found that the exponent $\beta \sim 0.3$ does not change with the size of the local region, and moreover its value is the same as that obtained for the global elastic modulus, suggesting that the material locally relaxes following the same process as in the bulk sample. However, the local relaxation times display a broad distribution, even if the stretching does not depend on this distribution and on the local features. Overall, the results of this work suggest that the dynamical relaxation is a very complex phenomenon that cannot be understood solely in terms of dynamical heterogeneity, but it also requires a full understanding of the non-trivial scale dependence due to the energy barriers that govern the relaxation process.

In a more recent study, Sun et al. investigated the relaxation mechanisms of different MGs by MD simulations. By studying the time evolution of the SISF at different temperatures, their results revealed two main kinds of relaxation mechanisms. In fact, the exponent β decreases from

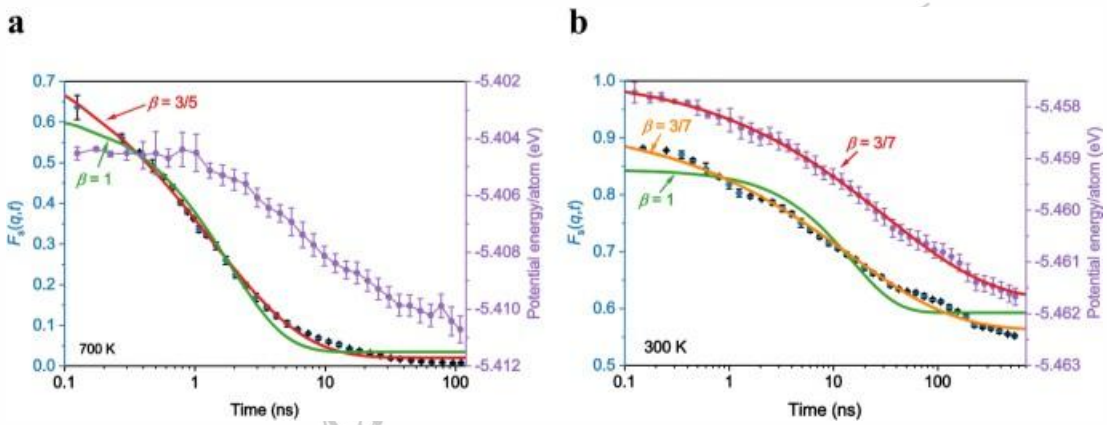

FIG. 10. Time evolution of SISF (diamonds) and potential energy (dots) for $Cu_{30}Zr_{70}$ obtained by MD simulations at (a) 700 K and (b) 300 K, showing distinct relaxation dynamics. Solid curves are fits of SISF and potential energy by KWW function with different values of the exponent β as indicated in the figure. Reprinted with permission from Ref. [125], copyright (2023).

1 far above T_g to 3⁄5 when approaching T_g and further to 3⁄7 when decreasing T far below T_g [125], as shown in Fig. 10. The exponent 3⁄7 was also found in stress-relaxation experiments of several MGs, suggesting a universal mechanism governing aging below T_g, and it can thus be considered as an indicator of the α relaxation. A microstructural explanation of β = 3⁄7 was given in terms of the evolution of the cavity volume during stress relaxation, which also follows a stretched exponential decay with the same exponent 3⁄7, and can thus be correlated to physical aging. Moreover, after aging the large cavities strongly decrease in number and size, and they can therefore be considered as seeds contributing to the relaxation dynamics. ~~These results evidence that the dynamics of a supercooled liquid is slower than that of the corresponding liquid, hence the name of stretched relaxation~~. However, upon decreasing temperature deeper in the glassy state, a recent experimental work reported a dynamical crossover from a stretched exponential with $\beta < 1$ in the supercooled liquid to a compressed exponential with $\beta > 1$ in the metastable glassy state for a Mg-based MG [126], essentially due to internal stress relaxation. A study of Wu al. by MD simulations on a $Cu_{50}Zr_{50}$ glass has shed some light on this intriguing phenomenon [91]. The authors studied the relaxation functions of different atomic environments, formed by icosahedral clusters of different connectivity, defined as the number of 12-fold coordinated Cu atoms that are neighbors of a given 12-fold coordinated Cu atom. Their results show that clusters with small connectivity, i.e. isolated icosahedra, are characterized by an exponent $\beta < 1$ with a liquid-like behavior, while icosahedra with large connectivity display a compressed relaxation with $\beta >$ 1,

more reminiscent of a solid-like behavior. In MGs, these two relaxation processes can coexist giving rise to a very complex and intriguing behavior. The crossover between these two dynamical behaviors strongly depend on temperature and on the wavenumber, thus on the length scale. For small values of the wavenumber, that is when the relaxation is probed on larger length scales, β is larger and the relaxation dynamics is faster, whereas for larger wavenumbers the dynamics is that of a supercooled liquid. The icosahedra with high connectivity form rigid structures that move in a viscous surrounding medium, driven by local internal stresses.

2. Secondary relaxations

As already stated in Sec. II, besides the primary relaxations other types of relaxations, called secondary relaxations, occur in amorphous materials at lower temperatures. The most outstanding of them is the slow β relaxation, which is linked to other properties of glasses, such as plasticity, aging, diffusion and crystallization. Secondary relaxations have been detected in experimental work, but a clear understanding of their microscopic origin is still lacking. In this respect, numerical simulations have contributed to elucidate some of the basic mechanisms responsible for these dynamical relaxations and also to assess why in some MGs β relaxation for instance is more prominent, showing a distinct peak, with respect to other MGs where only an excess wing is detected in the relaxation spectra. One of the main issues to capture the phenomenology of the β relaxation by atomistic simulations is the timescale limitation. In fact, as observed in experiments, β relaxation merges into α relaxation for temperatures close to T_g, but it can be distinguished from the main relaxation only deep in the glassy state where the dynamics becomes much slower, i.e. of the order of several microseconds. Thus, in order to fully observe the β relaxation the simulation time should be of the order of the microsecond, which requires a considerable amount of CPU time. Yu et al. performed extensive long-time MD simulations of DMS of different MGs to probe the β relaxation [34, 35]. Specifically, the cooling rate used to generate the glass structure was 2 to 3 orders of magnitude smaller than typical cooling rates used in MD, and the lower frequency of the sinusoidal strain was set to 10 MHz, allowing to simulate the dynamics up to the microsecond timescale. By analyzing the probability distribution of the atomic displacement vectors they found that MGs possessing a pronounced β peak have a larger fraction of fast-moving atoms and that the peaks of the displacement probability distribution correlate with the peak of the radial distribution function. As a consequence, atoms with large displacements rearrange in a cooperative manner by atomic jumps from one stable position to another by correlated hops. As schematically sketched

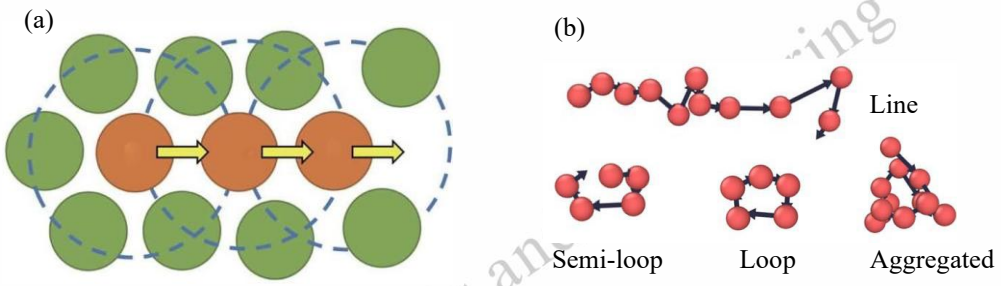

FIG. 11. (a) Scheme illustrating the mechanism of string-like motion. (b) Typical string-like configurations obtained from MD simulations. Reprinted with permission from Ref. [34], copyright (2017).

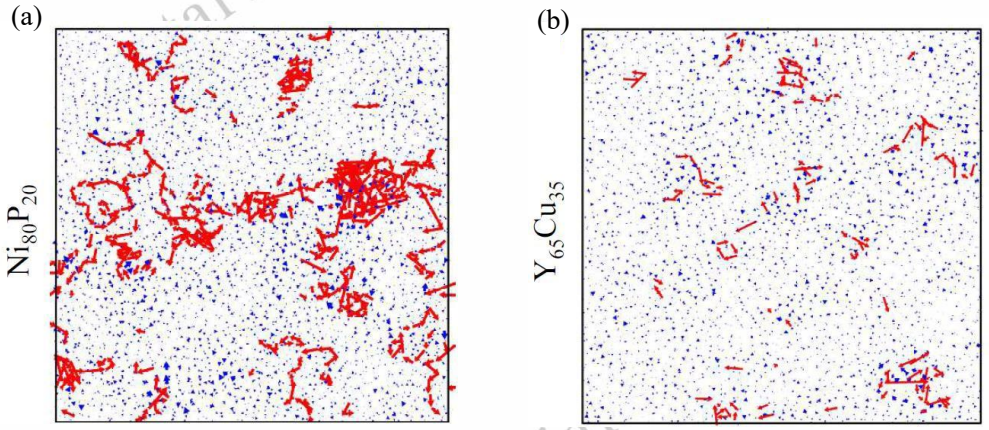

FIG. 12. Atomic displacements vectors for (a) $Ni_{80}P_{20}$ and (b) $Y_{65}Cu_{35}$, evidencing different degrees of string-like motions. Reprinted with permission from Ref. [35], copyright (2018).

in Fig. 11(a), one atom jumps to the position that is previously occupied by another atom in its nearest or secondary-neighbor shell. These correlated, cooperative hops manifest themselves in the form of string-like configurations that can be linear, loop-like or aggregated, as shown in Fig. 11(b), and which are sequentially activated in time. In MGs where the β peak is more prominent, the string-like configurations are more abundant and they are also larger in size compared to other metallic glasses that only exhibit an excess wing, where string-like motions are scarcer and strings are smaller. A typical comparison is shown in Fig. 12 for two prototypical MGs, e.g. $Ni_{80}P_{20}$, showing a well pronounced β peak, and $Y_{65}Cu_{35}$, which has an excess wing. It is evident that the dynamics of $Ni_{80}P_{20}$ is characterized by more string-like motions than $Y_{65}Cu_{35}$, and that the string-like configurations are longer. A previous study on MD of a Lennard-Jones binary mixture also associated the microscopic physical origin of the β relaxation to cooperative mechanisms rather than to localized atomic rearrangements [127]. Correlated motions resembling to string-like configurations of long chains of atoms were observed in a similar fashion as in Ref. [35], suggesting

that β relaxation is a cooperative phenomenon but it is not an extension of the α process. Thus, a correlation is established between string-like motion and β relaxation, and long strings have a larger contribution to the β relaxation. Moreover, the computed most probable time of the string-like motions, obtained by locating the peak of the time evolution of the number of atoms in a string normalized to the number of fast-moving atoms, matches quite well with the β relaxation time in a wide range of temperatures, further corroborating the link between string-like motion and β relaxation [35]. In order to understand why different MGs have different amount of string-like configurations and thus more or less pronounced β relaxations, Yu et al. showed that caging properties can influence the string-like motions, since atoms first have to escape from their cages in order to form a string-like configuration [35]. They monitored the cage breaking fraction of $Ni_{80}P_{20}$ and $Y_{65}Cu_{35}$ as a function of time. For $Ni_{80}P_{20}$ the cage breaking fraction is larger and increases more rapidly with time than for $Y_{65}Cu_{35}$, indicating that cages are easier to break. When cages break sooner, string-like cooperative motion sets in more easily at earlier times, yielding a sharper β relaxation. On the contrary, the presence of an excess wing rather than a peak for $Y_{65}Cu_{35}$ is due to the fact that atoms quit the cages late and do not have time to develop string-like motions since α relaxation occurs. In order to detect the β relaxation in atomistic simulations it is therefore necessary for the simulation time to be quite long to observe cage breaking and subsequent formation of string-like motion, which is possible only if the observation time reaches the microsecond timescale. String-like motions constitute therefore the basic event of β relaxation. It was shown by atomistic simulations and percolation analysis that the strings intertwine to form mobile clusters, which merge with their neighbors to form larger clusters until percolating through the whole space [128] . This percolation transition signals the occurrence of β relaxation and it has the same time and temperature dependence as the β relaxation. Percolation emerges universally when about 10% of the atoms are mobile.

It is widely recognized that the β relaxation is intrinsically linked to plasticity of MGs [32, 129, 130]. In a recent work, Zhou et al. implemented MD simulations with metadynamics in order to overcome the the timescale limititations of standard MD, as dicussed in Sec. III A 4, allowing to generate transition-state trajectories on experimentally relevant timescales, up to milliseconds [15]. They revealed that atoms participating in a STZ tend to form string-like motions and that the characteristic time of this motion corresponds to that of β relaxation. In some systems, due to their unique structural feature, such string-like motions are easily excited and not spatially confined, as in the case of $Al_{90}Sm_{10}$ MG, which exhibits a significant β relaxation feature. Such MG is also easily deformed on a macroscopic scale. In other systems, such as $Y_{65}Cu_{35}$ MG, the string-like

motion is suppressed by the large frozen environment. Therefore, the string-like collective motion is difficult to be excited and does not propagate, leading to a general lack of significant β relaxation and relatively less deformability at ambient temperature or at conventional time scales. Moreover, Yu et al. suggested that the activation energy of β relaxation in MGs is approximately equivalent to the potential energy barrier of STZs [24], a result already obtained in 2009 by Rodney and Schuh by atomistic simulations of a two-dimensional Lennard-Jones glass with the activation-relaxation technique used to explore the potential energy landscape [49]. These findings imply an intrinsic correlation between slow β relaxation, activation energy of STZs and the heterogeneous atomic structure of MGs. In this same spirit, Priezjev studied the mechanical relaxation of cyclically deformed binary Lennard-Jones glasses by MD simulations, and found that during the mechanical annealing the potential energy decreases, following a logarithmic decay with the number of cycles [67, 131], indicating a slow structural relaxation phenomenon. This mechanical annealing process is associated with intermittent plastic rearrangements, whose typical size is reduced as the system is relocated to progressively lower energy states upon cyclic loading [131]. Thus, atomistic simulations can provide physical insight into the microscopic origin of plastic deformation in MGs, and more generally in disordered materials.

Besides the slow β relaxation peak, DMS experiments have shown that the relaxation spectra become asymmetric near T_g developing an excess wing [132–134]. The microscopic origin of these excess wings is rather unclear, since they are difficult to be detected in atomistic simulations. Very recently, Guiselin et al. were able to probe the excess wing in a size-polydisperse mixture of soft repulsive spheres using the SMC method to generate glass equilibrium configurations combined with MD simulations up to very long time scales, of the order of 20 ms [135]. In fact, excess wings can only be accessed if the observation time is long enough to distinguish them from the main structural relaxation. They studied the dynamic susceptibility $\chi''(\omega)$ (Fourier transform of the SISF) and observed a development of a power-law by lowering temperature (Fig. 13(a)) with exponent 0.38. By analysis of the atomic structure, they found that the excess wing is due to a sparse population of relaxed, localized regions over broadly distributed timescales (Fig. 13(b)), whose relaxation time follows a power law with the same exponent 0.38 (Fig. 13(c)). The excess wing is interpreted as a broad underlying distribution of relaxation timesescales compressed by dynamic facilitation at long times. In this respect, we clearly see the strength of computer simulations to provide physical atomic explanations of phenomena that are experimentally inaccessible.

The β' relaxation is another kind of secondary relaxation observed in MGs whose underlying physical mechanisms are still unclear. By MD simulations of $Al_{90}La_{10}$ MG, Chang et al. have

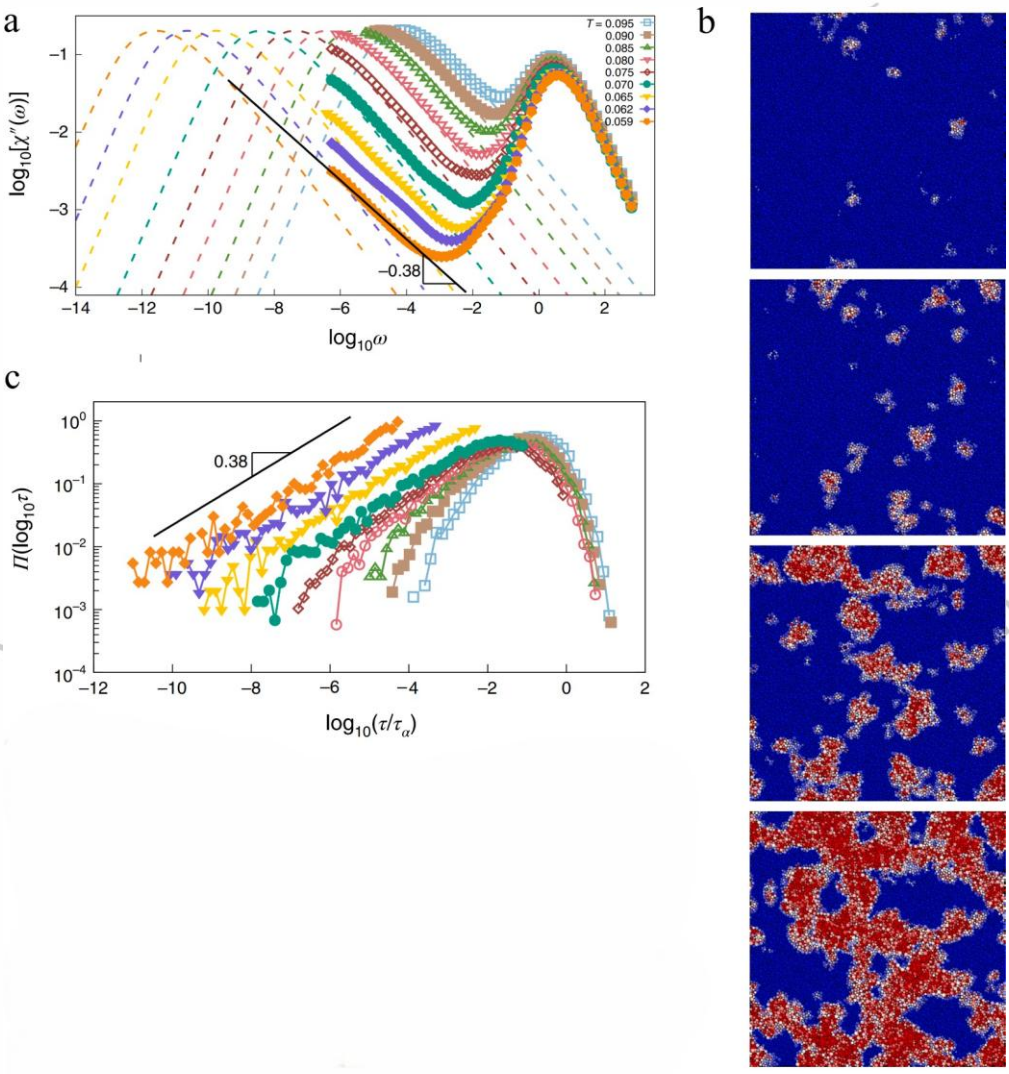

FIG. 13. (a) Relaxation spectra for the dynamic susceptibility at different temperatures as indicated in the legend. (b) Visualization of spatially heterogeneous and facilitated dynamics; particles are colored according to the bond-breaking correlation from blue (immobile) to red (relaxed). Reprinted with permission from Ref. [22] , copyright (2024).

revealed that the β' relaxation is due to the string-like diffusion of liquid-like atoms inherited from the high-temperature liquid and exhibiting a behavior similar to that in liquids, including comparable activation energies and low viscosities [136]. In a very recent work, Yu et al. also observed liquid-like clusters at low temperatures with a damping factor close to liquids and vanishing shear modulus, but with very low diffusion [137]. They state that these clusters are responsible for the β' relaxation. The presence of faster secondary relaxations has also been reported in thin metallic films of $Cu_{50}Zr_{50}$ by MD simulations [138]. In this system, a multistep relaxation is observed in the SISF, allowing to distinguish a fast β' mode and a slow β mode, due to the enhanced

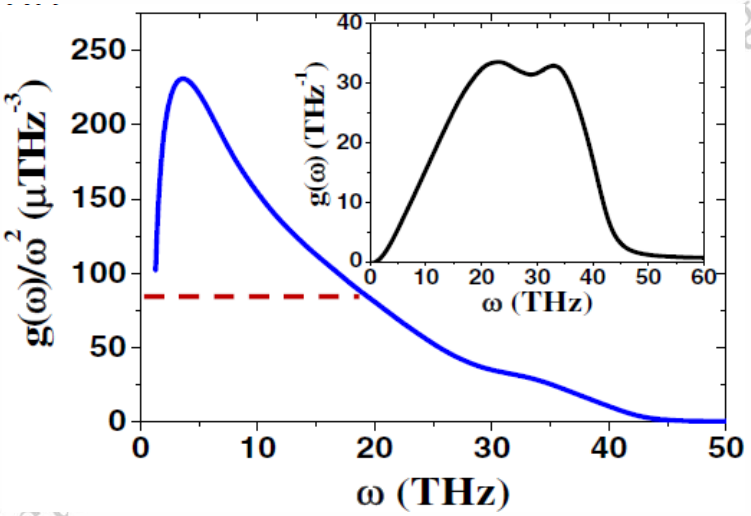

FIG. 14. Reduced vibrational density of states of $Cu_{50}Zr_{50}$ obtained by MD simulations. Reprinted with permission from Ref. [141] , copyright (2019).

mobility of the atoms near the surface. For the β relaxation the main atomic mechanism is identified with atoms jumping out of the cage region, while for the β' mode a cooperative string-like jump of the atoms is responsible for the relaxation process.

Another interesting manifestation of the secondary relaxations in MGs is represented by the *boson peak* phenomenon, already mentioned in Sec. II, which is an excess of low-frequency vibrational density of states, characteristic of disordered glassy solids, deviating from the Debye model [139, 140]. The explanation of the boson peak is still controversial, and its underlying physical mechanisms have not been well elucidated yet. Yang et al. performed MD simulations on a model $Cu_{50}Zr_{50}$ MG and calculated the vibrational density of states $g(\omega)$ by the Fourier transform of the velocity autocorrelation function [141]. They clearly saw the Boson peak by plotting the reduced vibrational density of states $g(\omega)/\omega^2$, as shown in Fig. 14. They found that all atoms participate to the low-frequency vibrations close to the boson peak, but the contribution of each atom to the boson peak strongly depends on the local SRO. They carried out an atomic-scale analysis, based on the orientational order, defined as a vector pointing from the center of each atom to the farthest vertex of its coordination polyhedron, and they found that the orientational order is the most probable direction of transverse vibrations at low frequencies. It turns out that the magnitude (length) of the orientational order parameter determines the boson peak intensity, and its spatial distribution produces the quasilocalized modes of the boson peak. In another work, Hu and Tanaka studied the miscroscopic origin of the boson peak with MD simulations by calculating the longitudinal and transverse dynamic structure factors over a wide range of frequencies [142].

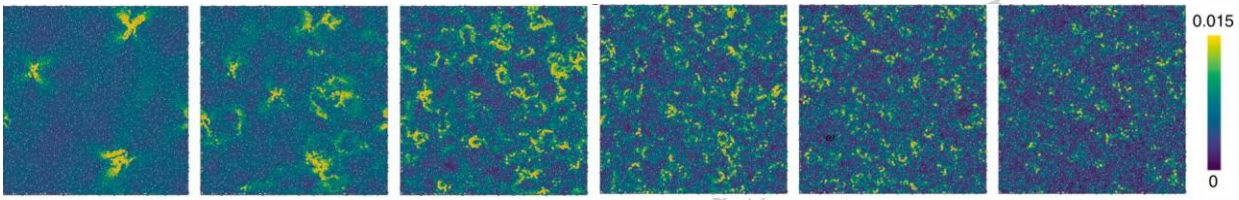

FIG. 15. Spatial distribution of the contribution of each particle to the reduced transverse vibrational density of states at different frequencies, evidencing different quasi-localized modes. Reprinted with permission from Ref. [22] , copyright (2024).

They showed that the boson peak originates from quasi-localized vibrations of string-like dynamical defects, which are coupled to transverse phonons. In Fig. 15 we can identify some examples of quasi-localized modes, such as four-leaf patterns, string- and ring-like patterns and more localized featureless patterns. Furthermore, these dynamical defects provide a common structural origin for the three most fundamental dynamic modes of glassy systems: the boson peak, fast β relaxation and slow structural relaxation. Interestingly, similar features originating from phonon softening mechanisms have been observed in strained glasses by Ren et al. using MC simulations to produce aged glasses, combined wuth MD runs to anneal the glasses at specified temperatures [143].

3. *Viscoelasticity and dynamical heterogeneities*

From these results it is evident that one of the most striking aspects of atomistic simulations is to probe the dynamical processes and the structural features at the atomic scale and to connect them to some observed phenomena. In this respect, this kind of simulations can provide a link between the microscopic dynamics and macroscopic quantities or properties. For example, a property that is related to dynamical relaxations is that of the viscoelasticity in MGs, which can be characterized by the dynamic moduli. A fundamental question is what determines viscoelasticity and dynamic moduli in glassy materials. Yu et al. addressed this issue by performing MD simulations of DMS on a model $Ni_{80}P_{20}$ MG [144]. They conducted a structural analysis based on atomic displacements and calculated the probability density function of the atomic displacements. This probability density evolves with temperature and it displays a peak that increases with temperature. The authors found that the temperature dependence of the peak position and that of the dynamic moduli is very similar, so that these two quantities are intrinsically correlated. On the other hand, systems with the same values of the dynamic moduli can show different dynamical heterogeneities, related to the large-displacement tail of the probability density function, i.e. to fast-moving atoms. They

concluded that, in spite of these structural differences, the dynamic moduli are primarily determined by the most probable value of the atomic displacements, and not by the dynamical heterogeneities induced by the faster atoms. In another work, Yu et al. investigated the atomic mechanisms of internal friction in a model $Cu_{65}Zr_{35}$ MG [53]. By again monitoring the distribution function of atomic displacements they established a correlation between internal friction and the concentration of faster atoms, thus suggesting that the internal friction, at variance with the dynamic moduli, is well affected by the dynamical heterogeneities. The fastest atoms tend to form clusterlike structures and act as cooperative avalanchelike excitations , triggering neighboring atoms in an intermittent stochastic fashion. Furthermore, the authors provided evidence that faster atoms are anticorrelated with atoms with full icosahedral symmetry. This finding is in agreement with more recent results of Lyu et al. related the atomistic processes responsible for viscoelasticity [86]. By performing MD simulations of DMS on $Cu_{64}Zr_{36}$, they showed that the spatial distribution of slow atoms matches quite well with that of atoms belonging to icosahedral clusters, as it can be clearly seen in Fig. 16. In fact, Cu-centered full icosahedra clusters are rather stable and have a low atomic mobility, contributing to the stored elastic energy during a loading cycle. On the other hand, the viscoelastic component is due to the atoms with higher mobilities that undergo irreversible inelastic displacements, and thus contribute to the dissipated energy. In the same work, DMS was simulated under different loading conditions and it was found that different elastic moduli have very contrasted dynamical behavior, but satisfy the dynamic correspondence principle. An example of DMS spectrum obtained with MD simulations at different frequencies for a given loading condition (constant volume) is presented in Fig. 17

Furthermore, several studies of dynamical relaxations in glasses have assessed that the presence of slow β relaxation is indicative of dynamical heterogeneities in the glass [16], as already discussed above. A thorough insight of dynamical heterogeneities at the atomic scale is very challenging from an experimental point of view. To overcome this limitation, atomistic simulations have been carried out in the last years to unravel the basic mechanisms of dynamical heterogeneities and to establish a link between the local structure and the macroscopic properties. The local structure of MGs contains both chemically and topologically favorable configurations and geometrically unfavored motifs [83, 145–147]. Local motifs such as icosahedra form the SRO and the medium-range order and constitute a rigid backbone with a dense packing in the glassy matrix, while unfavored motifs are characterized by a loose packing. Li et al. used the RMC method to generate reliable three-dimensional atomic structures for $Cu_{50}Zr_{50}$ and $Cu_{35}Zr_{65}$ to match the structure factor of X-ray diffraction experiments [148]. They found that the glass systems consist of a string-like backbone

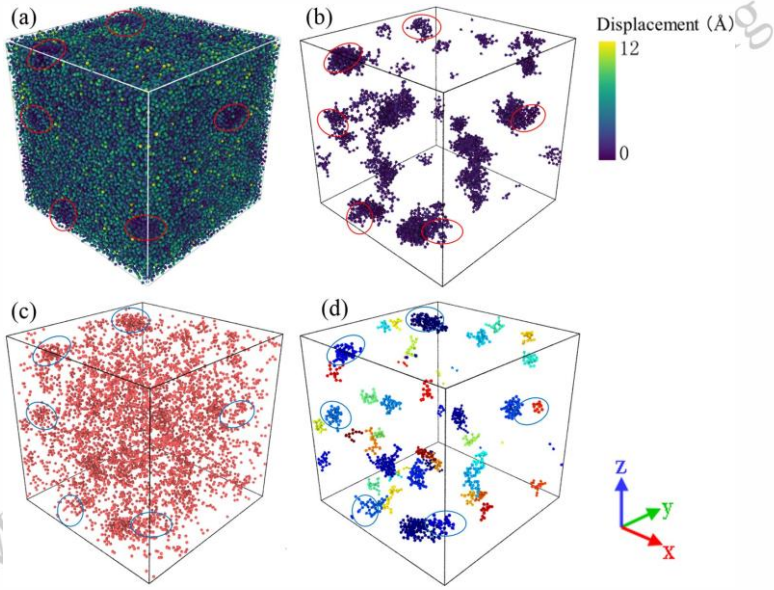

FIG. 16. (a) Snapshot of atomic displacement for cyclic loading of $Cu_{64}Zr_{36}$ at 800 K and 10 GHz by MD simulations. (b) Same as (a) when atoms with displacements < 1.4 Å and isolated atoms are removed. (c) Snapshot of Cu atoms at the center of icosahedra. (d) Same as (c) when isolated icosahedra are removed. Reprinted with permission from Ref. [86], copyright (2020).

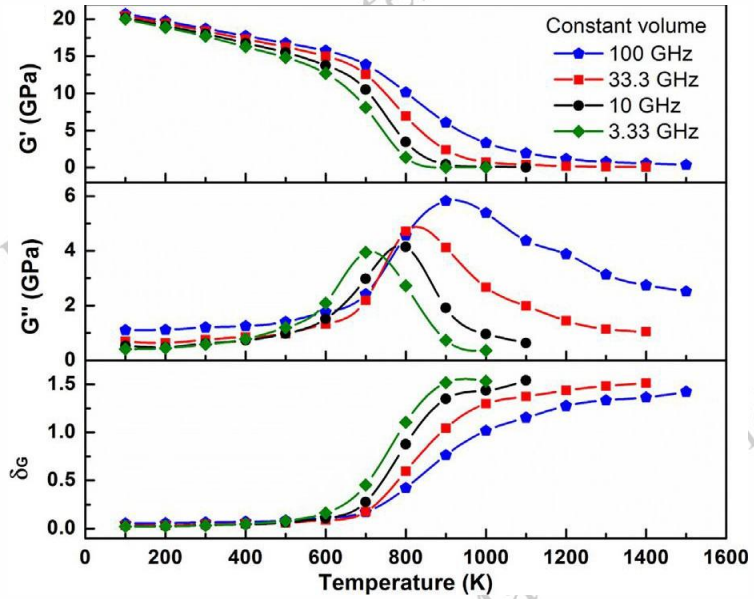

FIG. 17. Storage modulus G', loss modulus G'' and loss factor δ_G as a function of temperature for a constant volume cyclic deformation at different frequencies obtained by MD simulations on $Cu_{64}Zr_{36}$. Reprinted with permission from Ref. [86], copyright (2020).

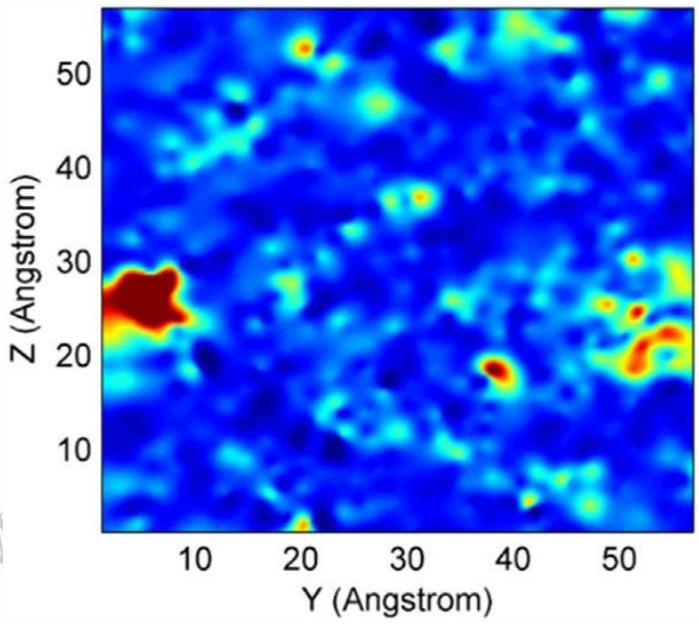

FIG. 18. Contour maps of a slice of the $Cu_{50}Zr_{50}$ MG representing the atomic non-affine displacement, revealing the inherent heterogeneity. Reprinted with permission from Ref. [149] , copyright (2016).

network formed by icosahedral clusters and a "liquid-like" structure filling in the remaining space. Hu et al. performed MD simulations combining isoconfigurational ensemble and atomic pinning methods in order to probe the dynamical heterogeneities in a $Cu_{50}Zr_{50}$ MG [149]. As it can be seen in Fig. 18, depicting a map of the non-affine displacement in a slice of the sample, flow units characterized by larger non-affine displacements can be clearly distinguished in the elastic matrix, indicating the emergence of dynamical heterogeneity already in the elastic regime. Thus, the structure of a MG is intrinsically inhomogeneous, with local soft spots that are prone to deform plastically. As mentioned before, since β relaxation is linked to the activation of STZs, MGs with prominent β relaxation will be characterized by heterogenous structures with more liquid-like zones. Fujita et al. performed MD simulations to investigate the mechanical behavior of $Cu_{45}Zr_{45}Ag_{10}$ MG subjected to iteration deformation in a nominally elastic region. It was found that cyclic deformation leads to the formation of irreversible STZs and a permanent uniform strain. The initiation of STZs is directly correlated with the atomic heterogeneity of the MG and the accumulated permanent strain has a linear relation with the number of STZs [150]. Moreover, the structural heterogeneity strongly affects the formation of STZs, since Ag-poor regions are more resistant to shear, while Ag-rich regions with looser atomic packing have weaker shear resistance to the initiation of STZs. In another work, Fujita et al. performed extensive MD simulations comparing two model systems, a binary alloy ($Cu_{50}Zr_{50}$) and a ternary alloy ($Cu_{45}Zr_{45}Ag_{10}$) [151]. They observed that the relaxation

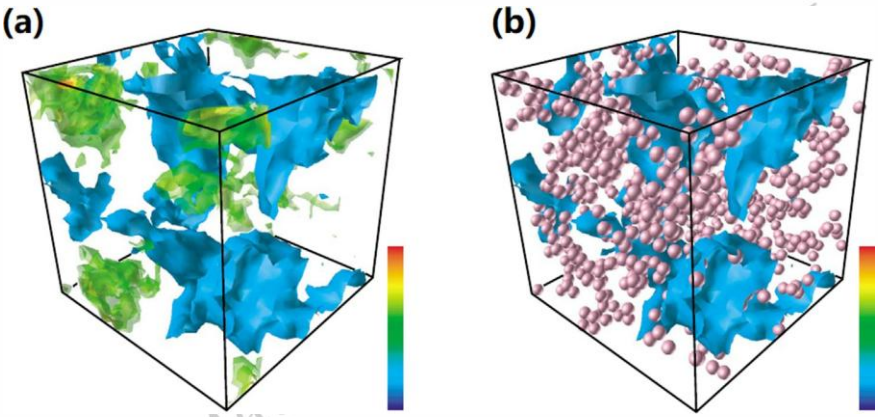

FIG. 19. Correlation between atomic mobility of Cu atoms and their local structural environments in $Cu_{45}Zr_{45}Ag_{10}$ at 800 K. The Cu atoms are sorted into 20 groups in the increasing order of their displacement. In each group, the percentage of full icosahedra and the number of coordinated Ag atoms are plotted with (a) 3D mean-square displacement map of all atoms based on propensity motion for a long time interval and (b) 3D map showing both isosurfaces of slow-dynamics regions and distribution of Ag atoms (balls). The slow-dynamics regions are apparently Ag-poor regions. The cube has the dimensions of $53 \times 53 \times 53$ Å^3; the color bars show the range from fast (top) to slow (bottom) dynamics. Reprinted with permission from Ref. [151], copyright (2010).

dynamics, as probed by the SISF, is very similar for the two systems, with comparable α relaxation times, in spite of the higher glass-forming ability found experimentally for the $Cu_{45}Zr_{45}Ag_{10}$ system. On the other hand, their results reveal a strong correlation between dynamic heterogeneity and chemical SRO for this ternary alloy. In fact, by addition of Ag the atomic motion becomes less cooperative in the ternary alloy, strongly increasing the dynamic heterogeneity. Interestingly, an intrinsic correlation between the chemical and dynamic heterogeneities manifests itself through a spatial partitioning in space between regions rich in Cu atoms with higher short-range icosahedral order, where the dynamics is slower, and regions rich of Ag atoms with a faster dynamics, as it can be seen in the snapshots of Fig. 19 showing the isosurfaces of slow-dynamics regions with small atomic displacements and fast-dynamics regions with larger atomic displacements. From Fig. 19(b) it is clear that the slow-dynamics regions are poor of Ag atoms, confirming the correlation between dynamic heterogeneity and chemical inhomogeneity. Moreover, this spatial partitioning due to the addition of Ag atoms can delay the crystallization kinetics and thus improve the glass-forming ability.

So far, we have presented key results of atomistic simulations for pure MGs, but experimentally glass composites are often considered. In fact, glass composites with a crystalline phase embedded

in a glassy matrix are generally believed to keep a tensile strength while improving ductility by delaying brittle fracture. A recent MD study on DMS and viscoelastic properties of MGs composites showed that dynamical relaxations and dynamic moduli exhibit a remarkably complex behavior, depending in a non-trivial manner on the spatial distribution of the microstructural heterogeneities and loading conditions, especially for the loss modulus [152]. This study revealed some fundamental structural and dynamic conditions for the occurrence of energy dissipation in pure and composite MGs, namely the existence of structural heterogeneity and local shear deformation, resulting in atomic shear motion between regions with different moduli.

V. CONCLUSIONS AND FUTURE DIRECTIONS

Numerical simulations have emerged as an indispensable tool for investigating dynamical relaxations in MGs. By employing techniques such as MD and MC, researchers have gained valuable insights into the mechanisms governing primary and secondary relaxation processes, providing a link between dynamical relaxations and structural heterogeneities in MGs. In spite of the progress made, challenges remain, particularly in bridging timescales and developing robust interatomic potentials and eventually hybrid approaches. Continued efforts to integrate experimental and computational approaches, along with advancements in machine learning, will be crucial for unlocking the full potential of metallic glasses in various applications. Below we propose some hints for future directions and perspectives in the use of numerical simulations for elucidating the still unresolved issues related to the understanding of dynamical relaxation processes in MGs.

1. **Extending timescales**

   As already discussed in Sec. III A 4, the main drawback of atomistic simulations, in particular MD, is the inability to describe phenomena over time exceeding few hundreds of nanoseconds. The SMC method is one of the possible routes to extend this timescale up to tens of microseconds. MD simulations with metadynamics have been very rarely used to study relaxation phenomena [15], even if accelerated MD techniques are in principle available in the literature [93, 153]. In this respect, it is of primary importance to push the accessible timescales further, since long-time dynamics is not just an extension of the existing one, but different features and phenomena can appear at longer timescales.

2. **Multiscale modeling**

   Atomistic simulations can describe relaxation phenomena at the atomic level, accessing the

elementary mechanisms and dynamical processes at the atomic scale. Nevertheless, the link between these atomic-level relaxation processes to real-life experimentally observed dynamical relaxation is still elusive. In order to bridge this gap, multiscale simulations can be carried out by for instance integrating MD with continuum mechanics or finite element models, or using coarse-grained modeling to study large-scale systems. Mesoscale models, such as phase-field or kinetic field theories, could also be applied to capture intermediate phenomena.

3. **Establishing a correlation between the glass structure and the atomic motions for relaxation dynamics**

   We have shown in Sec. IV that dynamical relaxations are determined by characteristic types of atomic motions and structural rearrangements. However, the link between these atomic motions and the surrounding glass structure is not completely clear yet. Atomistic simulations could be pushed forward to shed light on these connections.

4. **Effect of chemical composition on dynamical relaxations**

   MGs with different chemical compositions display various dynamical and mechanical properties. In particular, the effect of chemical composition on dynamical relaxations is not well understood. Ab-initio calculations can in principle be an appaopriate tool to investigate the effect of the composition at the atomic scale, but they are very limited in size and in time. MD simulations have less severe limitations of time and size, but they rely on the choice of the interatomic potentials. A promising approach would be to use machine-learning approaches to access longer timescales and larger system sizes.

5. **Incorporating Machine Learning (ML)**

   Linked to the previous point, ML techniques can be useful to develop more accurate and computationally efficient potentials, for example neural network potentials [154], and to speed up the MD simulations [155]. ML can serve to identify relaxation pathways, predict aging/rejuvenation behaviors and optimize material properties. Moreover, large datasets from simulations could be analyzed by ML to extract meaningful patterns related to relaxation and deformation [156].

6. **Understanding dynamical heterogeneities**

   In spite of the progress made by atomic-scale simulations to describe the structural features of dynamical heterogeneities, the link between slow dynamical relaxations and dynamical heterogeneities is still a matter of debate. A closer understanding of the microscopic origins

of the dynamical heterogeneity should be gained by developing appropriate analysis methods of the local glass structure coupled to the relaxation dynamics. ML approaches could again help to identify correlations between structural features and relaxation patterns.

7. **Developing a unified theory of relaxation processes**

   So far, numerical simulations have shed light on some essential basic atomic processes responsible for mechanical relaxations. However, a unifying theoretical framework to describe relaxation phenomena is still lacking. In fact, it is not yet established whether a given fundamental mechanism can account for the various relaxation processes in MGs. A recent study has opened the pathway to such a kind of study, by proposing a unified principle governing diverse dynamical processes across different disordered materials on the basis of a global order parameter, namely the inherent structure minimal displacement, to quantify the variability of configurations by a pattern-matching technique [157].

In conclusion, enormous progress has been achieved by numerical simulations concerning the understanding of the relaxation processes in MGs and the relation between structural characteristics and dynamic and mechanical properties. Due to the complexity of the behavior of glassy materials, computer simulations have still to face many challenges to describe dynamical phenomena over wider time and length scales, in order to provide more profound insights into the unique dynamics of these systems.

VI. BIBLIOGRAPHY

[1] M. Telford, The case for bulk metallic glasses, Materials Today **7**, 36 (2004).

[2] Q. Halim, N. A. N. Mohamed, M. R. M. Rejab, W. N. W. A. Naim, and Q. Ma, Metallic glass properties, processing method and development perspective: a review, The International Journal of Advanced Manufacturing Technology **112**, 1231 (2021).

[3] J. J. Kruzic, Bulk Metallic Glasses as Structural Materials: A Review, Advanced Engineering Materials **18**, 1308 (2016).

[4] W. H. Wang, C. Dong, and C. H. Shek, Bulk metallic glasses, Materials Science and Engineering R **44**, 45 (2004).

[5] J. Gu, X. Yang, A. Zhang, Y. Shao, S. Zhao, and K. Yao, Centimeter-sized Ti-rich bulk metallic

glasses with superior specific strength and corrosion resistance, Journal of Non-Crystalline Solids **512**, 206 (2019).

[6] M. Fan, A. Nawano, J. Schroers, M. D. Shattuck, and C. S. O'Hern, Intrinsic dissipation mechanisms in metallic glass resonators, Journal of Chemical Physics **151**, 144506 (2019).

[7] M. M. Khan, A. Nemati, Z. U. Rahman, U. H. Shah, H. Asgar, and W. Haider, Recent advancements in bulk metallic glasses and their applications: a review, Critical Reviews in Solid State and Materials Sciences **43**, 233 (2017).

[8] D. C. Hofmann and S. N. Roberts, Microgravity metal processing: from undercooled liquids to bulk metallic glasses, Microgravity **1**, 5003 (2015).

[9] M. Davidson, S. Roberts, G. Castro, R. P. Dillon, A. Kunz, H. Kozachkov, M. D. Demetriou, W. L. Johnson, S. Nutt, and D. C. Hofmann, Investigating amorphous metal composite architectures as spacecraft shielding, Advanced Engineering Materials **15**, 27 (2013).

[10] J. W. Qiao, H. L. Jia, and P. K. Liaw, Metallic glass matrix composites, Materials Science and Engineering: R: Reports **100**, 1 (2016).

[11] Z. F. Zhang, J. Eckert, and L. Schultz, Difference in compressive and tensile fracture mechanisms of $Zr_{59}Cu_{20}Al_{10}Ni_8Ti_3$ bulk metallic glass, Acta Materialia **51**, 1167 (2023).

[12] M. Chen, Mechanical Behavior of Metallic Glasses: Microscopic Understanding of Strength and Ductility, Annual Review of Materials Research **38**, 445 (2008).

[13] M. L. Falk and J. S. Langer, Deformation and failure of amorphous, solidlike materials, Annual Review of Condensed Matter Physics **2**, 353 (2011).

[14] D. S. Şopu, A. Stukowski, M. Stoica, and S. Scudino, Atomic-level processes of shear band nucleation in metallic glasses, Physical Review Letters **119**, 195503 (2017).

[15] Z.-Y. Zhou, Y. Sun, L. Gao, Y.-J. Wang, and H.-B. Yu, Fundamental links between shear transformation, β relaxation, and string-like motion in metallic glasses, Acta Materialia **246**, 118701 (2023).

[16] J. C. Qiao, Q. Wang, J.-M. Pelletier, H. Kato, R. Casalini, D. Crespo, E. Pineda, Y. Yao, and Y. Yang, Structural heterogeneities and mechanical behavior of amorphous alloys, Progress in Materials Science **104**, 250 (2019).

[17] W. H. Wang, Dynamic relaxations and relaxation-properties relationships in metallic glasses, Progress in Materials Science **1**, 429 (2019).

[18] D. V. Louzguine-Luzgin1, L. V. Louzguina-Luzgina, and A. Y. Churyumov, Mechanical Properties and Deformation Behavior of Bulk Metallic Glasses, Metals **3**, 1 (2013).

[19] N. Amigo, P. Cortès, and F. J. Valencia, Research on metallic glasses at the atomic scale: a systematic review, SN Applied Sciences **4**, 281 (2022).

[20] L. Berthier and D. R. Reichmann, Modern computational studies of the glass transition, Nature Review Physics **5**, 102 (2023).

[21] H. Liu, Z. Zhao, Q. Zhou, R. Chen, K. Yang, Z. Wang, L. Tang, and M. Bauchy, Challenges and opportunities in atomistic simulations of glasses: a review, Comptes Rendus Géoscience—Sciences de

la Planète **354**, 35 (2022).

[22] Z.-Y. Zhou, Q. Yang, and H.-B. Yu, Toward atomic-scale understanding of structure-dynamics-properties relations for metallic glasses, Progress in Materials Science **145**, 101311 (2024).

[23] K. Ngai, *Relaxation and diffusion in complex systems* (Springer Science & Businees Media, 2011).

[24] H.-B. Yu, W. H. Wang, and K. Samwer, The β relaxation in metallic glasses: an overview, Materials Today **16**, 183 (2013).

[25] H.-B. Yu, W. H. Wang, H. Y. Bai, and K. Samwer, The β relaxation in metallic glasses, National Science Review **1**, 429 (2014).

[26] P. Lunkenheimer, U. Schneider, R. Brand, and A. Loid, Glassy Dynamics, Contemporary Physics **41**, 15 (2000).

[27] M. Ediger and P. Harrowell, Perspective: Supercooled liquids and glasses, The Journal of Chemical Physics **137**, 080901 (2012).

[28] B. Ruta, E. Pineda, and Z. Evenson, Relaxation processes and physical aging in metallic glasses, Journal of Physics: Condensed Matter **29**, 503002 (2017).

[29] C. Liu, E. Pineda, and D. Crespo, Mechanical relaxation of metallic glasses: an overview of experimental data and theoretical models, Metals **5**, 1073 (2015).

[30] A. Burin, GLassy Materials and Disordered Solids: An Introduction to Their Statistical Mechanics, Physics Today **59**, 64 (2006).

[31] C. Liu, E. Pineda, D. Crespo, J. Qiao, Z. Evenson, and B. Ruta, Sub-T_g relaxation times of the alpha process in metallic glasses, Journal of Non-Crystalline Solids **471**, 322 (2017).

[32] H.-B. Yu, K. Samwer, Y. Wu, and W. H. Wang, Correlation between β relaxation and self-diffusion of the smallest constituting atoms in metallic glasses, Physical Review Letters **109**, 095508 (2012).

[33] H.-B. Yu, X. Shen, Z. Wang, L. Gu, W. H. Wang, and H. Bai, Tensile plasticity in metallic glasses with pronounced β relaxations, Physical Review Letters **108**, 015504 (2012).

[34] H.-B. Yu, R. Richert, and K. Samwer, Structural rearrangements governing Johari-Goldstein relaxations in metallic glasses, Science Advances **3**, e1701577 (2017).

[35] H.-B. Yu, M. Yang, Y. Sun, F. Zhang, J.-B. Liu, C. Wang, L. Ho, R. Richert, and K. Samwer, Fundamental Link between Relaxation, Excess Wing, and Cage-Breaking in Metallic Glasses, The Journal of Physical Chemistry Letters **9**, 5877 (2018).

[36] S. Y. Liang, F. Zhu, Y.-J. Wang, E. Pineda, T. Wada, H. Kato, and J. C. Qiao, On the kinetics of structural evolution in metallic glasses, International Journal of Engineering Science **205**, 104146 (2024).

[37] B. Wang, L. J. Wang, B. S. Shang, X. Q. Gao, Y. Yang, H. Y. Bai, M. X. Pan, W. H. Wang, and P. F. Guan, Revealing the ultra-low-temperature relaxation peak in a model metallic glass, Acta Materialia **195**, 611 (2020).

[38] A. Nogales, A. Sanz, and T. Ezquerra, On the role of the β process as precursor of the α relaxation in aromatic polyesters, Journal of Non-Crystalline Solids **352**, 4649 (2006).

[39] Y. Ding, F. Shi, X. Wang, Y. Bai, Z. Wang, and L. Hu, Evolution of coupling modes between α and β relaxations in metallic glass-forming liquids revealed by nano-calorimetry, Acta Materialia **266**, 119698 (2024).

[40] F. H. Stillinger, A topographic view of supercooled liquids and glass formation, Science **267**, 1935 (1995).

[41] W. W. H., Y. Yang, T. G. Nieh, and C. T. Liu, On the source of plastic flow in metallic glasses: Concepts and models, Intermetallics **67**, 81 (2015).

[42] Q. Wang, S. T. Zhang, Y. Yang, Y. Dong, C. T. Liu, and J. Lu, Unusual fast secondary relaxation in metallic glasses, Nature Communications **6**, 7876 (2015).

[43] Z. Wang, P. Wen, L. Huo, H. Bai, and W. H. Wang, Signature of viscous flow units in apparent elastic regime of metallic glasses, Applied Physics Letters **101**, 121906 (2012).

[44] C. A. Schuh, T. C. Hufnagel, and U. Ramamurty, Mechanical behavior of amorphous alloys, Acta Materialia **55**, 4067 (2007).

[45] Z. Wang, B. Yu, P. Wen, H. Bai, and W. H. Wang, Pronounced slow beta-relaxation in La-based bulk metallic glasses, Journal of Physics: Condensed Matter **23**, 142202 (2011).

[46] H.-B. Yu, K. Samwer, W. H. Wang, and H. Y. Bai, Chemical influence on β-relaxation and the formation of molecule-like metallic glasses, Nature Communications **4**, 1 (2013).

[47] B. Huang, Z. G. Zhu, T. P. Ge, H. Y. Bai, B. A. Sun, Y. Yang, C. T. Liu, and W. H. Wang, Hand in hand evolution of boson heat capacity anomaly and slow beta-relaxation in La-based metallic glasses, Acta Materialia **110**, 73 (2016).

[48] Z. Wen, P. Zhao, M. Pan, and W. H. Wang, Mechanical relaxation in supercooled liquids of bulk metallic glasses, Physica status solidi (a) **207**, 2693 (2010).

[49] D. Rodney and C. A. Schuh, Distribution of Thermally Activated Plastic Events in a Flowing Glass, Physical Review Letters **102**, 235503 (2009).

[50] Z. Lu, W. Jiao, W. H. Wang, and H. Bai, Flow unit perspective on room temperature homogeneous plastic deformation in metallic glasses, Physical Review Letters **113**, 045501 (2014).

[51] J. Wang, Y. Shen, J. Perepezko, and M. Ediger, Increasing the kinetic stability of metallic glasses, Acta Materialia **104**, 25 (2016).

[52] C. Wang, T. Yang, Y. Ma, Y. Sun, Y. Yin, L. Gong, L. Gu, P. Wen, P. Zhu, Y. W. Long, X. H. Yu, C. Q. Jin, W. H. Wang, and H. Bai, High stored energy of metallic glasses induced by high pressure, Applied Physics Letters **110**, 111901 (2017).

[53] H.-B. Yu and K. Samwer, Atomic mechanisms of internal friction in model metallic glasses, Physical Review B **90**, 144201 (2017).

[54] L. Z. Zhao, R. J. Xue, Z. Z. G., K. L. Ngai, W. H. Wang, and H. Y. Bai, A fast dynamic mode in rare earth based glasses, Journal of Chemical ¨Physics **118**, 1356 (2016).

[55] Z. G. Zhu, Y. Z. Li, Z. Wang, X. Q. Gao, P. Wen, H. Y. Bai, K. L. Ngai, and W. H. Wang, Compositional origin of unusual β-relaxation properties in La-Ni-Al metallic glasses, Journal of Chemical

Physics **141**, 084506 (2014).

[56] Q. Wang, J. J. Liu, Y. F. Ye, T. T. Liu, S. Wang, C. T. Liu, J. Lu, and Y. Yang, Universal secondary relaxation and unusual brittle-to-ductile transition in metallic glasses, Materials Today **20**, 293 (2017).

[57] S. Küchemann and Maaß, R., Gamma relaxation in bulk metallic glasses, Scripta Materialia **137**, 5 (2017).

[58] M. Allen and D. Tildesley, *Computer Simulations of Liquids* (Oxford University Press, New York, 2017).

[59] M. Allen, *Introduction to Molecular Dynamics Simulations* (published in Computational Soft Matter: From Synthetic Polymers to Proteins, Lecture Notes, Norbert Attig, Kurt Binder, Helmut Grubmüller, Kurt Kremer editors, NIC Series, Vol. 23, ISBN 3-00-012641-, 2004) pp. 1–28.

[60] H. Fehske, R. Schneider, and A. Weiße, *Computational many-particle physics, Vol. 739* (Springer, 2007).

[61] A. R. Leach, *Molecular Modelling; Principles and Applications* (Prentice Hall, New York, 2001).

[62] G. J. Martyna, M. L. Klein, and M. Tuckerman, Nosé–Hoover chains: the canonical ensemble via continuous dynamics, Journal of Chemical Physics **97**, 2635 (1996).

[63] M. Müser, S. V. Sukhomlinov, and L. Pastewka, Interatomic potentials: achievements and challenges, Advances in Physics: X **8**, 2093129 (2023).

[64] H. Jónsson and H. C. Andersen, Icosahedral Ordering in the Lennard-Jones Liquid and Glass, Physical Review Letters **60**, 2295 (1988).

[65] M. Li and W. L. Johnson, Instability of Matastable Solid-Solutions and Crystal to Glass-Transition, Physical Review Letters **70**, 1120 (1993).

[66] W. Kob, Computer Simulations of Supercooled Liquids and Glasses, Journal of Physics: Condensed Matter **11**, R85 (1999).

[67] N. V. Priezjev, Slow relaxation dynamics in binary glasses during stress-controlled, tension-compression cyclic loading, Computational Materials Science **153**, 235 (2018).

[68] J. F. Thomas, Failure of Cauchy Relation in Cubic Metals, Scripta Metallurgica **5**, 787 (1971).

[69] V. Heine, *Solid State Physics* (in Solid State Physics, Henry Ehrenreich, Frederick Seitz, David Turnbull editors, New York: Academic Press, 1970) pp. 249–263.

[70] M. S. Daw, S. M. Foiles, and M. I. Baskes, The embedded-atom method: a review of theory and applications, Materials Science Reports **9**, 251 (1993).

[71] V. Borovikov, M. I. Mendelev, and A. H. King, Effects of stable and unstable stacking fault energy on dislocation nucleation in nano-crystalline metals, Modelling and Simulation in Materials Science and Engineering **24**, 85017 (2016).

[72] Y. Kimura, T. Cagin, Y. Qi, and W. A. Goddard III, The Quantum Sutton-Chen Many-Body Potential for Properties of Fcc Metals, CalTech ASCI Technical Report 003 , California Institute of Technology, Pasadena (1998).

[73] A. Landa, P. Winblatt, A. Girshick, V. Vitek, A. Ruban, and H. Skriver, Development of Fin-

nis–Sinclair type potentials for Pb, Pb–Bi, and Pb–Ni systems: application to surface segregation, Acta Materialia **46**, 3027 (1998).

[74] M. Faruq, A. Villesuzanne, and G. Shao, Molecular-dynamics simulations of binary Pd-Si metal alloys: Glass formation, crystallisation and cluster properties, Journal of Non-Crystalline Solids **487**, 72 (2018).

[75] S. W. Kao, K. C. Yang, S. H. Wang, C. C. Hwang, P. Y. Lee, R. T. Huang, and T. S. Chin, Predicting the glass-forming-ability of alloys by molecular dynamics simulation: a working example of Ti–Co bulk metallic glasses, Japanese Journal of Applied Physics **48**, 061301 (2009).

[76] H. Wei, S. Wei, X. Zhu, and X. Lu, Investigation of structural, thermal, and dynamical properties of Pd–Au–Pt ternary metal nanoparticles confined in carbon nanotubes based on MD simulation, Journal of Physical Chemistry C **121**, 12911 (2017).

[77] C.-D. Wu, Atomistic simulation of nanoformed metallic glass, Applied Surface Science **343**, 153 (2015).

[78] M. Celtek and S. Sengul, The characterisation of atomic structure and glassforming ability of the Zr–Cu–Co metallic glasses studied by molecular dynamics simulations, Philosophical Magazine **98**, 783 (2018).

[79] F. Cleri and V. Rosato, Tight binding potentials for transition metal alloys, Physical Review B **48**, 22 (1993).

[80] J. Du, *Challenges in molecular dynamics simulations of multicomponent oxide glasses* (in Molecular Dynamics Simulations of Disordered Materials: From Network Glasses to Phase-Change Memory Alloys, Springer Series in Materials Science, Massobrio, C., Du, J., Bernasconi, M., and Salmon, P. S., editors, Springer International Publishing, Cham, 2015) pp. 157–180.

[81] S. Sundararaman, L. Huang, S. Ispas, and W. Kob, New interaction potentials for borate glasses with mixed network formers, Journal of Chemical Physics **152**, 104501 (2020).

[82] T. F. Soules, Computer simulations of glass structures, Journal of Non-Crystalline Solids **123**, 48 (1990).

[83] Y. Q. Cheng and E. Ma, Atomic-level structure and structure–property relationship in metallic glasses, Progress in Materials Science **56**, 379 (2011).

[84] R. Ranganathan, Y. Shi, and P. Keblinski, Frequency-dependent mechanical damping in alloys, Physical Review B **95**, 214112 (2017).

[85] T. Damart, D. Rodney, and A. Tanguy, Theory of harmonic dissipation in disordered solids, Physical Review B **95**, 0 (2017).

[86] G.-J. Lyu, J.-C. Qiao, Y. Yao, J.-M. Pelletier, D. Rodney, J. Morthomas, and C. Fusco, Dynamic correspondence principle in the viscoelasticity of metallic glasses, Scripta Materialia **174**, 39 (2020).

[87] P. Jalali and M. Li, Atomic size effect on critical cooling rate and glass formation, Physical Review B **71**, 014206 (2005).

[88] Y. Zhang, N. Mattern, and J. Eckert, Understanding the relationship between atomic structures and transport properties in $(Cu_{0.5}Zr_{0.5})_{100-x}Al_x$ (< 10) glass forming liquids: Molecular dynamics

simulations, Journal of Alloys and Compounds **514**, 141 (2012).

[89] Q. K. Li and M. Li, Atomic scale characterization of shear bands in an amorphous metal, Applied Physics Letters **88**, 241 (2006).

[90] M. Zink, K. Samwer, W. L. Johnson, and S. G. Mayr, Plastic deformation of metallic glasses: Size of shear transformation zones from molecular dynamics simulations, Physical Review B **73**, 172 (2006).

[91] Z. W. Wu, W. Kob, W.-H. Wang, and L. Xu, Stretched and compressed exponentials in the relaxation dynamics of a metallic glass-forming melt, Nature Communications **9**, 5334 (2018).

[92] X. Li, W. Song, K. Yang, N. M. A. Krishnan, B. Wang, M. Smedskjaer, J. C. Mauro, G. Sant, M. Balonis, and M. Bauchy, Cooling rate effects in sodium silicate glasses: bridging the gap between molecular dyanmics simulations and experiments, Journal of Chemical Physics **147**, 074501 (2017).

[93] A. Laio and M. Parrinello, Escaping free-energy minima, Proceedings of the National Academy of Sciences **99**, 12562 (2002).

[94] G. Fiorin, M. L. Klein, and J. Hénin, Using collective variables to drive molecular dynamics simulations, Molecular Physics **111**, 3345 (2013).

[95] S. Alamdari, J. Sampath, A. Prakash, L. D. Gibson, and J. Pfaendtner, *Efficient Sampling of High-Dimensional Free Energy Landscapes: A Review of Parallel Bias Metadynamics* (in Foundations of Molecular Modeling and Simulation , Conference Proceedings, Maginn, E. J. and Errington, J. editors, Springer, Singapore, 2021) pp. 123–141.

[96] S. Piana and A. Laio, A bias-exchange approach to protein folding, Journal of Physical Chemistry B **111**, 4553 (2007).

[97] L. Berthier, G. Biroli, D. Coslovich, W. Kob, and C. Toninelli, Finite-size effects in the dynamics of glass-forming liquids, Physical Review E **86**, 031502 (2012).

[98] P. Ganster, M. Benoit, W. Kob, and J.-M. Delaye, Structural properties of a calcium aluminosilicate glass from molecular-dynamics simulations: A finite size effects study, Journal of Chemical Physics **120**, 10172 (2004).

[99] P. G. Debenedetti and F. H. Stillinger, Supercooled liquids and the glass transition, Nature **410**, 259 (2001).

[100] M. Utz, P. G. Debenedetti, and F. H. Stillinger, Atomistic simulation of aging and rejuvenation in glasses, Physical Review Letters **84**, 1471 (2000).

[101] F. Arceri, F. P. Landes, L. Berthier, and G. Biroli, *Glasses and aging: A Statistical Mechanics Perspective* (Encyclopedia of Complexity and Systems Science (Living Reference), 2022).

[102] R. C. Welch, J. R. Smith, X. Potuzak, M. Guo, B. F. Bowden, T. J. Kiczenski, D. C. Allan, E. A. King, A. J. Ellison, and J. C. Mauro, Dynamics of Glass Relaxation at Room Temperature, Physical Review Letters **110**, 265901 (2013).

[103] P. Biswas, R. Atta-Fynn, and D. A. Drabold, Reverse Monte Carlo modeling of amorphous silicon, Physical Review B **69**, 195207 (2004).

[104] R. L. Mcgreevy, Reverse Monte Carlo modelling, Journal of Physics: Condensed Matter **13**, R877

(2001).

[105] Q. Zhou, T. Du, L. Guo, M. M. Smedskjaer, and M. Bauchy, New insights into the structure of sodium silicate glasses by force-enhanced atomic refinement, Journal of Non-Crystalline Solids **536**, 120006 (2020).

[106] H. Liu, L. Tang, N. M. A. Krishnan, G. Sant, and M. Bauchy, Structural percolation controls the precipitation kinetics of colloidal calcium– silicate–hydrate gels, Journal of Physics D: Applied Physics **52**, 315301 (2019).

[107] J. Hwang, A. M. Clausen, H. Cao, and P. M. Voyles, Reverse Monte Carlo structural model for a zirconium-based metallic glass incorporating fluctuation microscopy medium-range order data, Journal of Materials Research **24**, 3121 (2009).

[108] C. Liu, Z. Zhang, J. Ding, and E. Ma, On the reliability of using reverse Monte Carlo simulations to construct the atomic structure model of metallic glasses, Scripta Materialia **225**, 115159 (2023).

[109] H. Y. Playford, L. R. Owen, I. Levin, and M. G. Tucker, New insights into complex materials using reverse Monte Carlo modeling, Annual Review of Materials Research **44**, 429 (2014).

[110] A. Ninarello, L. Berthier, and D. Coslovich, Models and Algorithms for the Next Generation of Glass Transition Studies, Physical Review X **7**, 021039 (2017).

[111] M. E. J. Newman and G. T. Barkema, *Monte Carlo Methods in Statistical Physics* (Clarendon Press, Oxford, 1999).

[112] D. Gazzillo and G. Pastore, Equation of state for symmetric non-additive hard-sphere fluids: An approximate analytic expression and new Monte Carlo results, Chemical Physics Letters **159**, 388 (1989).

[113] T. S. Grigera and G. Parisi, Fast Monte Carlo algorithm for supercooled soft spheres, Physical Review E **63**, 045102 (2001).

[114] L. Berthier, E. Flenner, C. J. Fullerton, C. Scalliet, and M. Singh, Efficient swap algorithms for molecular dynamics simulations of equilibrium supercooled liquids, Journal of Statistical Mechanics: Theory and Experiment , 064004 (2019).

[115] G. Kapteijns, W. Ji, B. Brito, M. Wyart, and E. Lerner, Fast generation of ultrastable computer glasses by minimization of an augmented potential energy, Physical Review E **99**, 012106 (2019).

[116] C. Brito, E. Lerner, and M. Wyart, Theory for Swap Acceleration near the Glass and Jamming Transitions for Continuously Polydisperse Particles, Physical Review X **8**, 031050 (2018).

[117] L. Berthier and M. D. Ediger, How to "measure"a structural relaxation time that is too long to be measured?, Journal of Chemical Physics **153**, 044501 (2020).

[118] A. Pandey, P. Biswas, and D. A. Drabold, Inversion of diffraction data for amorphous materials, Scientific Reports **66**, 33731 (2016).

[119] S. Bottaro and K. Lindorff-Larsen, Biophysical experiments and biomolecular simulations: a perfect match?, Science **361**, 355 (2018).

[120] L. Berthier, F. Ghimenti, and F. van Wijland, Monte Carlo simulations of glass-forming liquids beyond

Metropolis, Journal of Chemical Physics **161**, 114105 (2024).

[121] J. C. Phillips, Stretched and exponential relaxation in molecular and electronic glasses, Reports of Progress in Physics **59**, 1133 (1996).

[122] M. D. Ediger, C. A. Angell, and D. J. Plazek, Supercooled Liquids and Glasses, Journal of Physical Chemistry **100**, 13200 (1996).

[123] R. Ranko, Heterogeneous dynamics in liquids: fluctuations in space and time, Journal of Physics: Condensed Matter **14**, R703 (2002).

[124] B. Shang, J. Rottler, P. Guan, and J.-L. Barrat, Local versus global stretched mechanical response in a supercooled liquid near the glass transition, Physical Review Letters **122**, 105501 (2019).

[125] Y.-T. Sun, R. Zhao, D.-W. Ding, Y.-H. Liu, H.-Y. Bai, L. M.-Z., and W.-H. Wang, Distinct relaxation mechanism at room temperature in metallic glass, Nature Communications **14**, 540 (2023).

[126] B. Ruta, Y. Chushkin, G. Monaco, L. Cipelletti, P. E., P. Bruna, V. M. Giordano, and M. Gonzalez-Silveira, Atomic-scale relaxation dynamics and aging in a metallic glass probed by X-ray photon correlation spectroscopy, Physical Review Letters **109**, 165701 (2012).

[127] Y. Cohen, S. Karmakar, I. Procaccia, and K. Samwer, The nature of the β-peak in the loss modulus of amorphous solids, European Physics Letters **100**, 36003 (2012).

[128] L. Gao, Y. Sun, and H.-B. Yu, Mobility percolation as a source of Johari-Goldstein relaxation in glasses, Physical Review B **108**, 014201 (2023).

[129] H.-B. Yu, W. Wang, H. Y. Bai, Y. Z. Wu, and M. Chen, Relating activation of shear transformation zones to β relaxations in metallic glasses, Physical Review B **81**, 220201(R) (2010).

[130] Q. Yang, C.-Q. Pei, H.-B. Yu, and T. Feng, Metallic Nanoglasses with Promoted β-Relaxation and Tensile Plasticity, Nano Letters **21**, 6051 (2021).

[131] N. V. Priezjev, Mechanical annealing and yielding transition in cyclically sheared binary glasses, Journal of Non-Crystalline Solids **590**, 121697 (2018).

[132] T. Bauer, P. Lunkenheimer, S. Kastner, and A. Loidl, Nonlinear Dielectric Response at the Excess Wing of Glass-Forming Liquids, Physical Review Letters **110**, 107603 (2013).

[133] P. Lunkenheimer, R. Wehn, U. Schneider, and A. Loidl, Glass Aging Dynamics, Physical Review Letters **95**, 055702 (2005).

[134] K. Duvvuri and R. Richert, Dielectric hole burning in the high frequency wing of supercooled glycerol, Journal of Chemical Physics **118**, 1356 (2003).

[135] B. Guiselin, C. Scalliet, and L. Berthier, Microscopic origin of excess wings in relaxation spectra of supercooled liquids, Nature Physics **18**, 468 (2022).

[136] C. Chang, H. P. Zhang, R. Zhao, F. C. Li, P. Luo, M. Z. Li, and H. Y. Bai, Liquid-like atoms in dense-packed solid glasses, Nature Materials **21**, 1240 (2022).

[137] H.-B. Yu and Q. Wang, Liquid-like clusters in glassy solids as a unique state of matter: Dissipative but non-diffusive, Next Materials **3**, 100168 (2024).

[138] Q. L. Bi, Y. J. Lü, and W. H. Wang, Multiscale relaxation dynamics in ultrathin metallic glass-forming

films, Physical Review Letters **120**, 155501 (2018).

[139] V. K. Malinovsky, V. N. Novikov, P. P. Parshin, A. P. Sokolov, and M. G. Zemlyanov, Universal Form of the Low-Energy (2 to 10 meV) Vibrational Spectrum of Glasses, Europhysics Letters **11**, 43 (1990).

[140] B. Frick and D. Richter, The Microscopic Basis of the Glass Transition in Polymers from Neutron Scattering Studies, Science **267**, 1939 (1995).

[141] J. Yang, Y.-J. Wang, E. Ma, A. Zaccone, L. H. Dai, and M. Q. Jiang, Structural Parameter of Orientational Order to Predict the Boson Vibrational Anomaly in Glasses, Physical Review Letters **122**, 015501 (2019).

[142] Y.-C. Hu and H. Tanaka, Origin of the boson peak in amorphous solids, Nature Physics **18**, 669 (2022).

[143] S. Ren, H.-X. Zong, X.-F. Tao, Y.-H. Sun, B.-A. Sun, D.-Z. Xue, X. Ding, and W. H. Wang, Boson-peak-like anomaly caused by transverse phonon softening in strain glass, Nature Communications **12**, 5755 (2021).

[144] H.-B. Yu, R. Richert, and K. Samwer, Correlation between Viscoelastic Moduli and Atomic Rearrangements in Metallic Glasses, The Journal of Physical Chemistry Letters **7**, 3747 (2016).

[145] E. Ma, Tuning order in disorder, Nature Materials **14**, 547 (2015).

[146] D. B. Miracle, A structural model for metallic glasses, Nature Materials **3**, 697 (2004).

[147] H. W. Sheng, W. K. Luo, F. M. Alamgir, J. M. Bai, and M. E., Atomic packing and short-to-medium-range order in metallic glasses, Nature **439**, 419 (2006).

[148] M. Li, C. Z. Wang, S. G. Hao, M. J. Kramer, and K. M. Ho, Structural heterogeneity and medium-range order in Zr_xCu_{100-x} metallic glasses, Physical Review B **80**, 184201 (2009).

[149] Y. C. Hu, P. F. Guan, M. Z. Li, C. T. Liu, Y. Yang, H. Y. Bai, and W. H. Wang, Unveiling atomic-scale features of inherent heterogeneity in metallic glass by molecular dynamics simulations, Physical Review B **93**, 214202 (2016).

[150] T. Fujita, Z. Wang, Y. Liu, H. Sheng, W. Wang, and C. M., Low temperature uniform plastic deformation of metallic glasses during elastic iteration, Acta Materialia **60**, 3741 (2012).

[151] T. Fujita, P. F. Guan, H. W. Sheng, A. Inoue, T. Sakurai, and M. W. Chen, Coupling between chemical and dynamic heterogeneities in a multicomponent bulk metallic glass, Physical Review B **81**, 140204(R) (2010).

[152] G. J. Lyu, J. C. Qiao, Y. Yao, Y.-J. Wang, J. Morthomas, C. Fusco, and D. Rodney, Microstructural effects on the dynamical relaxation of glasses and glass composites: A molecular dynamics study, Acta Materialia **220**, 117293 (2021).

[153] A. F. Voter, Hyperdynamics: Accelerated Molecular Dynamics of Infrequent Events, Physical Review Letters **78**, 3908 (1997).

[154] R. Martin-Barrios, R. Navas-Conyedo, X. Zhang, Y. Chen, and J. Gulín-González, An overview about neural networks potentials in molecular dynamics simulation, Quantum Chemistry **124**, e27389 (2024).

[155] P. Friederich, F. Häse, J. Proppe, and A. Aspuru-Guzik, Machine-learned potentials for next-generation matter simulations., Nature Materials **20**, 750 (2021).

[156] E. D. Cubuk, R. J. S. Ivancic, S. S. Schoenholz, D. J. Strickland, A. Basu, Z. S. Davidson, J. Fontaine, J. L. Hor, Y.-R. Huang, Y. Jiang, N. C. Keim, K. D. Koshigan, J. A. Lefever, T. Liu, X.-G. Ma, D. J. Magagnosc, E. Morrow, C. P. Ortiz, J. M. Rieser, A. Shavit, T. Still, Y. Xu, Y. Zhang, K. N. Nordstrom, P. E. Arratia, R. W. Carpick, D. J. Durian, Z. Fakhraai, D. J. Jerolmack, D. Lee, J. Li, R. Riggleman, K. T. Turner, A. G. Yodh, D. S. Gianola, and A. J. Liu, Structure-property relationships from universal signatures of plasticity in disordered solids, Science **358**, 1033 (2017).

[157] H.-B. Yu, L. Gao, J.-Q. Gao, and K. Samwer, Universal origin of glassy relaxation as recognized by configuration pattern matching, National Science Review **11**, nwae091 (2024).